

คำอรรถมาตรฐานของเทคนิคเอ็ม-99เอ็ม SESTAMIBI ในการตรวจกล้ามเนื้อหัวใจ  
ด้วยเครื่องสเปค/ซีที



นางสาวอนมาร์ ชเว

จุฬาลงกรณ์มหาวิทยาลัย

CHULALONGKORN UNIVERSITY

บทคัดย่อและแฟ้มข้อมูลฉบับเต็มของวิทยานิพนธ์ตั้งแต่ปีการศึกษา 2554 ที่ให้บริการในคลังปัญญาจุฬาฯ (CUIR)  
เป็นแฟ้มข้อมูลของนิสิตเจ้าของวิทยานิพนธ์ ที่ส่งผ่านทางบัณฑิตวิทยาลัย

The abstract and full text of theses from the academic year 2011 in Chulalongkorn University Intellectual Repository (CUIR)  
are the thesis authors' files submitted through the University Graduate School.

วิทยานิพนธ์นี้เป็นส่วนหนึ่งของการศึกษาตามหลักสูตรปริญญาวิทยาศาสตรมหาบัณฑิต

สาขาวิชาอายุรเวชศาสตร์ ภาควิชารังสีวิทยา

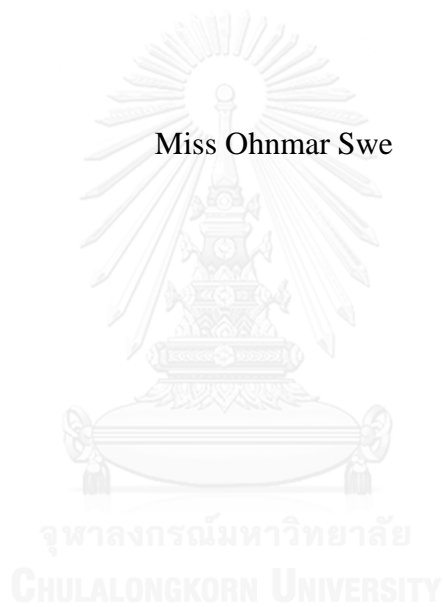
คณะแพทยศาสตร์ จุฬาลงกรณ์มหาวิทยาลัย

ปีการศึกษา 2557

ลิขสิทธิ์ของจุฬาลงกรณ์มหาวิทยาลัย

STANDARDIZED UPTAKE VALUE OF  $^{99m}\text{Tc}$ -  
SESTAMIBI IN MYOCARDIAL PERFUSION SPECT/CT

Miss Ohnmar Swe



A Thesis Submitted in Partial Fulfillment of the Requirements  
for the Degree of Master of Science Program in Medical Imaging

Department of Radiology

Faculty of Medicine

Chulalongkorn University

Academic Year 2014

Copyright of Chulalongkorn University

Thesis Title	STANDARDIZED UPTAKE VALUE OF <sup>99m</sup> Tc-SESTAMIBI IN MYOCARDIAL PERFUSION SPECT/CT
By	Miss Ohnmar Swe
Field of Study	Medical Imaging
Thesis Advisor	Associate Professor Anchali Krisanachinda, Ph.D

---

Accepted by the Faculty of Medicine, Chulalongkorn University in Partial Fulfillment of the Requirements for the Master's Degree

..... Dean of the Faculty of Medicine  
(Associate Professor Sophon Napathorn, MD)

THESIS COMMITTEE

..... Chairman  
(Associate Professor Supatporn Tepmongkol, MD)

..... Thesis Advisor  
(Associate Professor Anchali Krisanachinda, Ph.D)

..... External Examiner  
(Professor Franco Milano, Ph.D)

จุฬาลงกรณ์มหาวิทยาลัย  
CHULALONGKORN UNIVERSITY

ออนมาร์ ชเว : ค่าอัพเทคมาตรฐานของเทคนิคเซียม-99เอ็ม SESTAMIBI ในการตรวจกล้ามเนื้อหัวใจด้วยเครื่องสเปค/ซีที (STANDARDIZED UPTAKE VALUE OF  $^{99m}\text{Tc}$ -SESTAMIBI IN MYOCARDIAL PERFUSION SPECT/CT) อ.ที่ปริกษาวิทยานิพนธ์หลัก: รศ. ดร. อัญชลี กฤษณจินดา, 88 หน้า.

ค่าอัพเทคมาตรฐานในการศึกษาการทำงานของกล้ามเนื้อหัวใจด้วยเทคนิคเซียม 99 เอ็ม เซสตามิบี สเปคซีทีสามารถประเมินจากอัตราส่วนของความแรงกัมมันตรังสีที่วัดได้ต่อพื้นที่ผิวผนังและกัมมันตรังสีที่ฉีดให้ผู้ป่วยโดยคำนวณเป็นเปอร์เซ็นต์ เมื่อกัมมันตรังสีกระจายสม่ำเสมอทั่วร่างกาย ค่าดังกล่าวมีค่าเท่ากับ 1 วัตถุประสงค์ของการศึกษานี้เพื่อหาค่าอัพเทคมาตรฐาน ในผู้ป่วยที่มารับการศึกษาการทำงานของกล้ามเนื้อหัวใจ และมีการสแกนด้วยโปรโตคอลของเครื่อง สเปค ซีที วัสดุที่ใช้ประกอบด้วยเครื่อง สเปค ซีที เทคนิคเซียม 99 เอ็ม เซสตามิบีหุ่นจำลองทรงกระบอกกลวงบรรจุสารละลาย และหุ่นจำลองส่วนนอกของผู้ป่วยพร้อมอวัยวะภายในช่องอก และ หุ่นจำลองเรขาคณิตแทนสิ่งแปลกปลอม มีการศึกษาในผู้ป่วยที่มีการทำงานของกล้ามเนื้อหัวใจปกติ 20 ราย และผิดปกติ 27 ราย โดยมีผลการศึกษาจากวิธีการตรวจสอบหัวใจโดยระบบฟลูออโรสโคปมาเปรียบเทียบ มีการประเมินปัจจัยแก้ไข 2 ปัจจัยคำนวณจากการศึกษาในหุ่นจำลองทั้ง 3 แบบ และนำไปใช้ในผู้ป่วย ค่าเฉลี่ยของปัจจัยทั้งสองมีค่า 4875 ครั้งต่อนาทีต่อเมกะเบคเคอเรล และ 0.565 ตามลำดับ ในการประมวลภาพด้วยโปรแกรม e-soft จากผู้ผลิต ค่าเฉลี่ยและค่าเบี่ยงเบนมาตรฐานของค่าอัพเทคมาตรฐาน ในผู้ป่วยที่มีการทำงานของกล้ามเนื้อหัวใจปกติมีค่า  $8.15 \pm 1.21$  ในช่วงที่ไม่ได้ออกกำลังกาย และมีค่า  $8.00 \pm 1.5$  เมื่อออกกำลังกาย ในผู้ป่วยที่มีการทำงานของกล้ามเนื้อหัวใจผิดปกติค่าอัพเทคมาตรฐานมีค่า  $9.47 \pm 2$  ในช่วงที่ไม่ได้ออกกำลังกาย และมีค่า  $8.92 \pm 2$  เมื่อออกกำลังกาย เมื่อใช้ซอฟต์แวร์ Image J ค่าเฉลี่ยและค่าเบี่ยงเบนมาตรฐานของค่าอัพเทคมาตรฐาน ของกล้ามเนื้อหัวใจที่มีหลอดเลือด 3 หลอดเลือดมาเลี้ยง มีค่า  $7.70 \pm 1.2$ ,  $8.15 \pm 1.1$ ,  $7.61 \pm 1.3$  ในช่วงที่ไม่ได้ออกกำลังกาย และมีค่า  $7.67 \pm 1.2$ ,  $8.04 \pm 1.5$ ,  $7.56 \pm 1.2$  เมื่อออกกำลังกาย ในผู้ป่วยที่มีการทำงานของกล้ามเนื้อหัวใจปกติ ในผู้ป่วยที่มีการทำงานของกล้ามเนื้อหัวใจผิดปกติ มีการเปรียบเทียบกับผลการศึกษาจากวิธีการตรวจสอบหัวใจ โดยระบบฟลูออโรสโคป โดยคำนวณค่า Z-score ซึ่งได้จากการเปรียบเทียบกับค่าอัพเทคมาตรฐานของคนปกติ โดยใช้โปรแกรม Image J ช่วยในการวัดพื้นที่ส่วนต่างๆของหัวใจ ค่าอัพเทคมาตรฐานมีค่า negative predictive value สูงกว่า วิธีการแปลผลด้วยตาในการคัดกรองการทำงานที่ผิดปกติออก ค่าความจำเพาะ 74% ค่าความไว 58% และค่าความถูกต้อง 67% ของค่าอัพเทคมาตรฐานที่ศึกษาในกล้ามเนื้อหัวใจ มีค่าสูงกว่าวิธีการเดิม ซึ่งมีค่าความจำเพาะ 51% ค่าความไว 52% และค่าความถูกต้อง 51% ความรุนแรงของรอยโรคสามารถสังเกตได้จากค่า Z-score ที่เป็นลบ การศึกษานี้มีประโยชน์ในกรณีที่มีการประเมินปริมาณเลือดมาเลี้ยงกล้ามเนื้อหัวใจของชายล่างเป็นตัวเลข SUV ได้โดยแบ่งตามพื้นที่กล้ามเนื้อหัวใจที่หลอดเลือดมาเลี้ยง

ภาควิชา รังสีวิทยา

ลายมือชื่อนิพนธ์ .....

สาขาวิชา ฉายาเวชศาสตร์

ลายมือชื่อ อ.ที่ปริกษาหลัก .....

ปีการศึกษา 2557

# # 5674094130 : MAJOR MEDICAL IMAGING

KEYWORDS: SPECT/CT / STANDARDIZED UPTAKE VALUE / QUANTITATIVE STUDY / MYOCARDIAL PERFUSION / 99MTC- SESTAMIBI

OHNMAR SWE: STANDARDIZED UPTAKE VALUE OF <sup>99m</sup>Tc-SESTAMIBI IN MYOCARDIAL PERFUSION SPECT/CT. ADVISOR: ASSOC. PROF. ANCHALI KRISANACHINDA, Ph.D, 88 pp.

The standardized uptake value (SUV) of <sup>99m</sup>Tc SESTAMIBI in myocardial perfusion imaging is the measured activity normalized for surface area and injected dose. As a reference, if the dose were uniformly distributed over the entire body, the value everywhere would be one. The purpose of this study is to determine the standardized uptake value in myocardial perfusion imaging patients using quantitative SPECT/ CT protocol. The materials in this study include SPECT/CT system, <sup>99m</sup>Tc SESTAMIBI, one hollow cylindrical phantom, two anthropomorphic phantoms with inserts, twenty patients with normal myocardial perfusion scan and twenty-seven abnormal patients who underwent coronary angiogram. Conversion Factor and recovery coefficient were calculated using the above phantoms and then applied to the patients. The average conversion factor and recovery coefficient were 4875 CPM/MBq and 0.565 respectively. In using the e-soft reconstruction algorithm, the SUV for mean and SD in normal myocardial perfusion scan for rest and stress studies were  $8.15 \pm 1.21$  and  $8.00 \pm 1.5$  respectively. Using Image J software method, the average SUV for three vessels of the heart, LAD, LCX and RCA, in normal myocardial perfusion imaging were  $7.70 \pm 1.2$ ,  $8.15 \pm 1.1$ ,  $7.61 \pm 1.3$  in rest scan and  $7.67 \pm 1.2$ ,  $8.04 \pm 1.5$ ,  $7.56 \pm 1.2$  in stress scan. By comparing the two methods with T-test, the SUV for normal patients were not significantly different. For abnormal scan, z scoring method is used to define the cut off score between normal SUV and abnormal SUV from image J segmentation method. Coronary angiography result was used as a gold standard to define diagnostic index. The score result on each segment of left ventricle had been compared with MPI retrospective report. The results showed that SUV had higher negative predictive value for eliminating perfusion defects. Specificity of 74%, sensitivity of 58% and accuracy of 67% of SUV study for the heart were higher than conventional myocardial perfusion imaging (51%, 52%, 51%), respectively. The severity of defect can be observed by looking at the negative score level. The benefit of this study is to obtain absolute quantification for myocardium perfusion measurement in SUV values.

Department: Radiology

Student's Signature .....

Field of Study: Medical Imaging

Advisor's Signature .....

Academic Year: 2014

## ACKNOWLEDGEMENTS

The success of this thesis depends on the contribution of many people. First of all, I wish to express gratitude and deepest appreciation to Associate Professor Dr. Anchali Krisanachinda, Department of Radiology, Faculty of Medicine, Chulalongkorn University, my major adviser, for her supervision, guidance, encouragement and invaluable advice during the whole study. I wish to express appreciation to Associate Professor Dr. Supatporn Tepmonkol, and Mr. Panya Pasawang, Section of Nuclear Medicine, Department of Radiology, Faculty of Medicine Chulalongkorn University and King Chulalongkorn Memorial Hospital, Thai Red Cross Society, my co-advisors for their help in the experiment, assistance and suggestion in this research. I gratefully acknowledge the member of my Thesis committee: Associate Professor Dr. Tawatchai Chaiwatanarat, M.D, Nuclear Medicine Division, Department of Radiology, Faculty of Medicine, Chulalongkorn University and external examiner, Professor Franco Milano, University of Florence, Italy for their comments and valuable suggestion to this study. I would like to greatly thank to medical physicists, nuclear medicine physicians and Radiological Technologists, Section of Nuclear Medicine, King Chulalongkorn Memorial Hospital, Thai Red Cross Society, especially, Mr. Tanawat Sontrapornpol, Mr. Chatchai Navikhacheewin, for their help and suggestions in this study. I am also thankful for all teachers, lecturers and staffs in the Master of Science Program in Medical Imaging, Faculty of Medicine, Chulalongkorn University, for their unlimited teaching of knowledge throughout whole study.

Finally, my grateful is forwarded to the support by Chulalongkorn University ASEAN Scholarship Program, Kingdom of Thailand and the Republic of the Union of Myanmar for their financial support. I also express my gratefulness to every member in my family for their supports, valuable encouragement during the course study.

## CONTENTS

	Page
THAI ABSTRACT .....	iv
ENGLISH ABSTRACT.....	v
ACKNOWLEDGEMENTS .....	vi
CONTENTS.....	vii
LIST OF TABLES .....	x
LIST OF FIGURES .....	xii
LIST OF ABBREVIATION .....	xiii
CHAPTER I INTRODUCTION.....	1
1.1 Background and rationale .....	1
1.2 Research Objective .....	3
1.3 Definition .....	3
CHAPTER II LITERATURE REVIEWS Overview of myocardial perfusion .....	6
2.1 Principle of myocardial perfusion SPECT .....	6
2.1.1 Gated SPECT Imaging .....	7
2.1.2 Data acquisition .....	8
2.1.3 Photon attenuation .....	8
2.1.4 Partial volume effect (PVE) .....	10
2.2 SPECT reconstruction .....	11
2.2.1 Iterative reconstruction.....	12
2.2.2 Quantitative Analysis .....	12
2.2.3 SPECT/CT.....	13
2.3 Review of related literatures .....	14
CHAPTER III RESEARCH METHODOLOGY .....	18
3.1 Research design .....	18
3.2 Research design model .....	18
3.3 Conceptual framework.....	19
3.4 Research question .....	20
3.4.1 Primary research question .....	20

	Page
3.4.2 Secondary research question .....	20
3.5 Key words .....	20
3.6 The sample .....	20
3.7 Materials .....	21
3.7.1 Single Photon Emission Computed Tomography/ Computed Tomography (SPECT/CT) .....	21
3.7.2 Cylindrical uniform phantom .....	21
3.7.3 Anthropomorphic thorax and heart phantom .....	22
3.7.4 Torso phantom with hollow sphere inserts (IEC) .....	23
3.8 Methods .....	24
3.8.1 SPECT/CT daily QC [APPENDIX C] .....	24
3.8.2 The preparation of cylindrical uniform phantom .....	24
3.8.3 The preparation of anthropomorphic thorax and heart phantom.....	24
3.8.4 The preparation of hollow sphere phantom.....	25
3.8.5 Patient study .....	25
3.8.6 Data analysis.....	26
3.8.6.1 Conversion Factor (CF) .....	26
3.8.6.2 Recovery coefficient.....	26
3.8.6.3 Standardized Uptake Value .....	27
3.9 Statistical analysis.....	27
3.10 Ethical Consideration.....	27
3.11 Expected benefits.....	27
CHAPTER IV RESULTS.....	28
4.1 The conversion factor (CF).....	28
4.2 The recovery coefficient (RC) .....	29
4.2.1 The RC of the anthropomorphic phantom with six sphere inserts .....	29
4.2.2 The RC of anthropomorphic heart and thorax phantom.....	31
4.3 Anthropomorphic Heart and Thorax Phantom with 5 cc defect.....	33
4.4 Standardized Uptake Value of normal myocardial perfusion scans .....	38



	Page
4.5 Standardized Uptake Value of abnormal myocardial perfusion scan.....	46
4.6 Relation between SUV and MPI.....	59
CHAPTER V DISCUSSION AND CONCLUSION .....	63
5.1 Discussion.....	63
5.2 Conclusion .....	65
5.3 Limitations .....	66
5.4 Recommendation .....	66
REFERENCES .....	67
APPENDIX A.....	70
APPENDIX B.....	71
APPENDIX C.....	73
VITA.....	88



## LIST OF TABLES

Table	Page
Table 2. 1 CT number of various tissues .....	10
Table 2. 2 SUVs for compartments of IEC phantom for SPECT and PET .....	16
Table 4. 1 The conversion factors (CPM/MBq) from 3 acquisitions .....	28
Table 4. 2 The value of the recovery coefficient of six spheres .....	30
Table 4. 3 The average value of recovery coefficient.....	30
Table 4. 4 . The recovery coefficients of the anthropomorphic thorax phantom.....	31
Table 4. 5. The recovery coefficients of the anthropomorphic thorax phantom.....	32
Table 4. 6 The relation between relative true activity concentration and measured activity concentration of percent defect.....	34
Table 4. 7. The relation between relative true activity concentration and measured activity concentration of percent defect by applying different RC in AcC .....	36
Table 4. 8. The relation between relative true activity concentration and measured activity concentration of percent difference by applying different RC in (%) .....	36
Table 4. 9 SUV for Rest normal myocardial perfusion scan in female patients.....	39
Table 4. 10 SUV for Stress normal myocardial perfusion scan in female patients .....	40
Table 4. 11 SUV for Rest normal myocardial perfusion scan in male patients.....	41
Table 4. 12 SUV for Stress normal myocardial perfusion scan in male patients .....	42
Table 4. 13 The example of rest SUV for normal myocardial perfusion scan by using Image J .....	44
Table 4. 14 (a)(b) Example of rest SUV in LAD, LCX and RCA and for normal scan and average SUV in normal patients .....	45
Table 4. 15 Average SUV for rest normal myocardial perfusion scan .....	49
Table 4. 16 Average SUV for stress normal myocardial perfusion scan.....	50
Table 4. 17 The result of Rest SUV in 27 abnormal myocardial perfusion scan .....	51
Table 4. 18 The result of Rest SUV in 27 abnormal myocardial perfusion scan for 20 segments (cont.).....	52
Table 4. 19 The result of Rest score in 27 abnormal myocardial perfusion scan .....	53

Table 4. 20 The result of Rest score in 27 abnormal myocardial perfusion scan for 20 segments (Cont.) .....	54
Table 4. 21 The result of stress SUV in 27 abnormal myocardial perfusion scan.....	55
Table 4. 22 The result of stress SUV in 27 abnormal myocardial perfusion scan for 20 segments (cont.) .....	56
Table 4. 23 The result of stress score in 27 abnormal myocardial perfusion scan .....	57
Table 4. 24 The result of stress score in 27 abnormal myocardial perfusion scan for 20 segments (cont.) .....	58
Table 4. 25 The diagnostic indexes of MPI compare with CAG results .....	59
Table 4. 26 The diagnostic indexes of SUV for stress compared with CAG .....	59
Table 4. 27 Percent specificity, sensitivity and accuracy of SUV and MPI for three vessels (LAD, LCX and RCA) .....	60
Table 4. 28 Percent specificity, sensitivity and accuracy for LAD, LCX and RCA of the heart in SUV (stress) and MPI.....	60

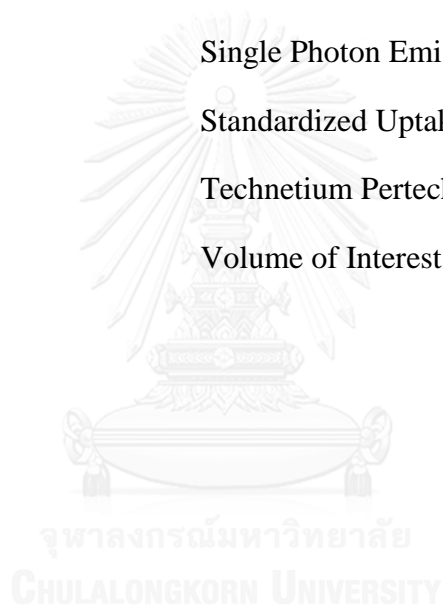
## LIST OF FIGURES

Figures	Page
Figure 1. 1 Myocardial perfusion imaging QPS surface rendering and polar map display images.....	1
Figure 2. 1 The plot of recovery coefficient values against object diameter .....	11
Figure 2. 2 Comparison of quantitative PET ( $^{18}\text{F}$ ) and SPECT ( $^{99\text{m}}\text{Tc}$ ) images.....	15
Figure 2. 3 SPECT quantification obtained from postmortem images .....	17
Figure 3. 1 Research design model .....	18
Figure 3. 2 Conceptual framework .....	19
Figure 3. 3 SPECT/CT system.....	21
Figure 3. 4 Cylindrical uniform phantom .....	22
Figure 3. 5 Anthropomorphic thorax and heart phantom and myocardial chamber ....	22
Figure 3. 6 Torso phantom with six hollow sphere inserts .....	23
Figure 4. 1. The reconstructed image of cylinder uniformity phantom .....	28
Figure 4. 2 Reconstructed image of the IEC phantom with six sphere inserts .....	29
Figure 4. 3 Sphere volume vs recovery coefficient .....	31
Figure 4. 4 The reconstructed images of myocardial phantom, Left image .....	32
Figure 4. 5 Measured volume versus Recovery Coefficient.....	33
Figure 4. 6. Measured percentage of defect in heart phantom.....	37
Figure 4. 7. Reconstructed images with 5 cc defect .....	37
Figure 4. 8 Auto-contour ISO 50 % ROI for normal myocardial perfusion scan.....	38
Figure 4.9 Myocardial Perfusion SPECT 20-Segment Scoring. Diagrammatic.....	43
Figure 4. 10 The sample image of 20 segments drawn by Image J software .....	47
Figure 4. 11 Percent specificity, sensitivity and accuracy for three main vessels .....	61
Figure 4. 12 Percent specificity, sensitivity and accuracy for LAD in 27 patients.....	61
Figure 4. 13 Percent specificity, sensitivity and accuracy for left circumflex.....	62
Figure 4. 14 Percent specificity, sensitivity and accuracy for right coronary in 27 patients. ....	62

## LIST OF ABBREVIATION

Abbreviation	Terms
%	Percent
3D	Three Dimension
AcC	Activity Concentration
BW	Body weight
COR	Center of Rotation
CPM	Counts per minute
CT	Computed Tomography
CTDI	Computed Tomography Dose Index
CF	Conversion Factor
FWHM	Full width at half-maximum
g	Gram
HU	Housfield Units
IEC	International Electro-technical Commission
Inj: act	Injected Activity
kVp	Kilovoltage peak
LAD	Left Anterior Descending
LCX	Left Circumflex
mA	Milliampere
MBq	Megabecquerel
mL	Milliliter
mm	Millimeter
max	Maximum

NaI(Tl)	Sodium iodide thallium activated
NEMA	National Electrical Manufacturers Association
PMTs	Photomultiplier tubes
Pt. no.	Patient number
ROI	Region of Interest
RC	Recovery Coefficient
RCA	Right Coronary Artery
Seg: no.	Segments number
SPECT	Single Photon Emission Computed Tomography
SUV	Standardized Uptake Value
$^{99m}\text{TcO}_4^-$	Technetium Pertechnetate
VOI	Volume of Interest



# CHAPTER I

## INTRODUCTION

### 1.1 Background and rationale

Myocardial perfusion imaging (MPI) using single-photon emission tomography (SPECT) is a widely used noninvasive modality in the diagnosis of coronary artery disease (CAD) and for assessing the functional significance of coronary stenosis. However, current techniques for assessing myocardial perfusion studies generally rely on visual interpretation and analysis of relative tracer activity within the myocardial regions. (1)

Visual interpretation of SPECT perfusion images used short-axis and vertical long-axis are divided into 20 segments. Segments were scored by using a five-point scoring system (where 0 is normal; 1 is equivocal; 2 is moderate; 3 is severe reduction of radioisotope uptake; 4 is absence of detectable radiotracer in the segment).

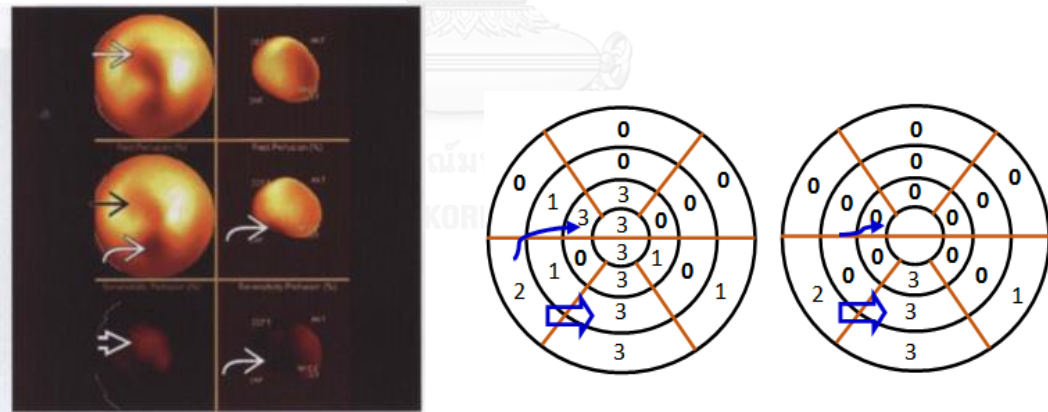


*Figure 1. 1 Myocardial perfusion imaging QPS surface rendering and polar map display images*

In conventional relative perfusion imaging, the polar map display results are normalized to the highest activity observed. Most of the techniques rely on maximal counts derived from radial sectors of reconstructed short axis normalized by count values in regions of peak intensity. Patients with multi-vessel disease, although qualitative and relative quantitative analysis may identify the most

severely stenosed coronary artery, less severely stenosed arteries may not be identified without an absolute measure of the radionuclide uptake in the myocardium. Non-homogeneous photon attenuation in the thorax is one of the most important drawbacks of MPI, limiting the diagnostic accuracy and interpretive confidence. Several studies (Da Silva AJ et al, Willowson K et al) have shown the strong prognostic value of SPECT MPI. Nevertheless, attenuation artifacts have remained an important issue(2).

To overcome these problems and to better discriminate perfusion defects from artifacts, several methods have been proposed. With the advent of integrated SPECT/CT technology, the SPECT data is obtained in the same coordinate frame as the CT, image fusion has significantly improved. CT-AC has several advantages over external radionuclide sources for AC, such as higher photon flux and no influence from the SPECT radionuclide, no decay of transmission source, and shorter scan times(3).

In quantitative Single Photon Emission Computed Tomography (SPECT), the calculation of absolute radionuclide concentrations allows useful information to be obtained regarding in vivo function. Such data have not been readily available from SPECT studies, due to the degrading effects of attenuated and scattered photons. In addition, quantitative values from structures that have a diameter less than approximately three times the total system spatial resolution can also be affected by the partial volume effect. X-ray computed tomography (CT) has been used as an accurate tool to perform patient specific, non-uniform attenuation correction. This method relies on the use of an attenuation ( $\mu$ ) map which is created from the CT data using a conversion from Hounsfield units to attenuation coefficients(4).

Absolute quantification is, to make an absolute measurement of MBq/cc in a specified region. The standardized uptake value is the measured activity normalized for surface area or body weight and injected dose. As a reference, if the dose were uniformly distributed over the entire body, the value everywhere would be  $\sim 1.0$ . This process is compromised by photon scatter, photon attenuation, and partial volume artifact. However, with the advent of SPECT/CT, the efforts to develop truly quantitative SPECT have considerably gained(5).



$$SUV = \frac{\text{Activity concentration in VOI (MBq/cc)}}{\text{Injected Dose (MBq) / Body Weight (g)}}$$

## 1.2 Research Objective

To determine the standardized uptake value of myocardial perfusion in patients using a quantitative SPECT/ CT protocol.

## 1.3 Definition

### Single Photon Emission Computed Tomography (SPECT)

An imaginary modality allows to visualize functional information about a patient's specific internal organ or body system using the distribution of radionuclide in the target organ.

### Computed Tomography

Computed Tomography is a technique for constructing images of the structures at a particular depth within the body done by taking several x-ray images at different angles and then using a computer to reconstruct and analyze the resulting images.

### Myocardial perfusion

It is non-invasive imaging that shows how well blood flows through the heart muscle. It can show area of the heart muscle that are not getting enough blood flow.

### Myocardial ischemia

Myocardial ischemia is the status of an imbalance between oxygen supply and demand, and the extent and severity of ischemia assessed by myocardial perfusion imaging.

## Myocardial infarction

A heart attack (myocardial infarction) is usually caused by a blood clot, which stops the blood flowing to a part of the heart muscle.

## Becquerel

The Becquerel is a unit of radioactivity corresponding to one disintegration per second.

(1 Ci=  $3.7 \times 10^{10}$  disintegration per second).

## Absolute quantification (Activity concentration)

Absolute quantification is the concentration of radioactivity within a given volume of tissue in absolute units, e.g. megabecquerel per cubic centimeter.

## Standardized Uptake Value (SUV)

It is also known as the dose uptake ratio (DUR). As the name suggests it is a mathematically derived ratio of tissue radioactivity concentration at a point in time  $C(T)$  and the injected dose of radioactivity per kilogram of the patient's body weight(6).

## Recovery coefficient (RC)

It represents the ratio of the apparent concentration to the true concentration for the correction of the partial volume effect.

## $^{99m}\text{Tc}$ Sestamibi (methoxyisobutylisonitrile)

It is a myocardial perfusion agent that is indicated for detecting coronary artery disease by localizing myocardial ischemia and infarction, in evaluating myocardial function and developing information for use in patient management decisions.

## Coronary angiogram

A coronary angiogram is a procedure that uses X-ray imaging to see the heart's blood vessels.

## Spatial resolution

Spatial resolution refers to a camera's ability to spatially resolve two sources of radioactivity as separate items.



## CHAPTER II

### LITERATURE REVIEWS

#### Overview of myocardial perfusion

SPECT Myocardial Perfusion Imaging using  $^{99m}\text{Tc}$ -sestamibi is an accepted test for the evaluation of patients with coronary artery disease. SPECT imaging performed after stress reveals the distribution of the radiopharmaceutical, and therefore the relative blood flow to the different regions of the myocardium. Comparing stress images to a further set of images obtained at rest aids in diagnosis. Physical interaction of photons with the patient by Compton scattering or photoelectric effect and the effect of spatial resolution by collimator detector are significant factors affecting the quality of SPECT images, importance to cardiac SPECT(7).

#### 2.1 Principle of myocardial perfusion SPECT

Myocardial perfusion is recorded in at least three projections: anterior, 45 LAO and a steep LAO view with the patient in the supine position. Although imaging of the object in different projections can give some information about the depth of the structure, tomographic scanners make a precise assessment of the depth of a structure in an object. In cardiac imaging, this translates to the ability to better distinguish normal from hypo perfused myocardial distribution. It is primarily attributed associated with the improved diagnosis result over planar image and quantitation in early clinically.

Three dimensional display generally falls into two categories: volume rendering and surface rendering. Volume rendering offers the advantage of visualizing an object in 3D without having to explicitly identify the surface. The most common type of volume rendering in SPECT is the technique of maximum intensity projection (MIP) developed by Wallis and Miller. In this approach, the reconstructed trans axial slices are first stacked to form a 3D tomographic volume.

$^{99m}\text{Tc}$  Sestamibi is a myocardial perfusion imaging agent that offers significant advantages over thallium-201 (Tl-201) for myocardial perfusion imaging.  $^{99m}\text{Tc}$  Sestamibi is monovalent hydrophilic cations, lipophilic and facilitates entry into cells. Uptake is dependent on blood flow, plasma and mitochondrial derived membrane electrochemical gradients, cellular pH and intact energy pathways. Following intravenous injection is cleared from the blood by the liver, concentrated in the gallbladder and excreted through the common bile duct into the GI tract. The initial high liver uptake does not allow the inferior wall to be seen clearly early post injection and requires waiting 30–60 min following resting or pharmacologic stress injection to get adequate visualization. Clearance post exercise is rapid and image acquisition can be started as soon as 10–20 min following injection(8).

### 2.1.1 Gated SPECT Imaging

Cardiac gating allows heart motion and contraction to be resolved by dividing the projection into discrete time parts coupled with the cardiac cycle. The electrocardiogram is used to determine the heart rate and the onset contraction at the QRS complex. The cardiac cycle is divided a set number of predetermined time intervals, called frames and counts collected during each frame are directed to a different projection set. Counts are directed into the first frame during the initial  $T/N$  seconds after the QRS complex is detected, where  $N$  is the number of frames and  $T$  is the length in second of the cardiac cycle. Then, counts are directed into the second frame for the second  $T/N$  seconds, and so on. This is repeated for each heartbeat during the acquisition, at every angle. At the end of the acquisition, there are  $N$  sets of complete projection images. When these are reconstructed, the result is  $N \times 3 \times D$  sets of slides showing the heart at  $N$  points during the cardiac cycle. These four-dimensional data allow 3D analysis of motion and myocardial thickening, as well as perhaps enabling better discrimination of the extent and location of perfusion abnormalities. It is possible to obtain quantitative functional information from gated perfusion SPECT Images. Local variables such as left ventricular volumes, mass and ejection fraction can be calculated. Local properties

of wall motion and myocardial thickening are also obtainable; these can then be displayed using either polar maps or 3D graphics. Most commercially available programs for quantifying cardiac function are fully 3D approaches, which start by detecting endocardial and epicardium surface points through the cardiac cycle(9).

### 2.1.2 Data acquisition

Data acquired by rotation the detector head around the long axis of the patient over 180 or 360 degree, while 180 data collection is commonly used for cardiac study since it minimizes the effects of attenuation and variation of resolution with depth. Data collection can be made in either continuous motion or step and shoot mode. In continuous acquired data are later binned into the number of segments equal to the number of projection desired. In the step and shoot mode, the detector moves around the patient at selected incremental angles and collects the data for the projection at each angle.

Other variable factors are the size of the pixel, the average number of counts collected in each pixel, and the number of views obtained. In general, this pixel size should be less than one-third the system resolution. The number of counts in each pixel is also related to the system resolution; the higher the resolution, the lower the number counts obtained per pixel. Pixels 6 to 6.5 mm in size have proved to be adequate for cardiac SPECT. This size is obtained by using a 64x64 pixel matrix for systems with a field of view of 38 to 40 cm. 64 projections over 180 degrees are preferred but 32 projections are used with satisfactory results(10).

### 2.1.3 Photon attenuation

Gamma ray photons are attenuated in body tissue while passing through a patient. The degree of attenuation depends on the photon energy, the thickness of the tissue and the linear attenuation coefficient of the photons in tissue. Techniques are employed to correct for attenuation. In one method, an uncorrected image is taken and the thickness of tissue through which the photons are attenuated of estimated. Using constant linear attenuation coefficient of the photons in tissue, each pixel data is correct to this equation to reconstruct the image.

$$I_t = I_0 e^{-\mu x}$$

If the photon beam initial intensity  $I_0$  passes through an absorber of thickness  $x$ , then the transmitted beam  $I_t$  is given by exponential equation, where  $\mu$  is the linear attenuation coefficient of absorbing for photon of interest and has a unit of  $\text{cm}^{-1}$ . The factor of  $e^{-\mu x}$  represents the factor of the photon transmitted. Assumption of a constant linear attenuation coefficient can be useful for symmetric organs with similar tissue density, and it is not valid for several organs such as the heart, cause of the close proximity to other organs. Gamma ray traversing different thicknesses of various body tissues may be detected within the photo peak and therefore a constant correction factor may not be sufficient for attenuation correction. Attenuation corrections are not applied to SPECT images for reasons of complexity of the problem. The detectors collect the transmission data to correct for attenuation in emission data. However, one should keep in mind that there is a likelihood of spillover of scattered high-energy photon into the low energy window. The transmission data are used to calculate the attenuation factor to apply to emission data.

The CT image is represented in terms of normalized CT numbers or Hounsfield units; CT image contains pixel values that are related to the linear attenuation coefficient at that point in the patient, calculated from the mean energy of the x ray photons used to generate the CT image. After the computer calculates the linear attenuation coefficient for each pixel via filtered back-projection, the values are normalized to the value of water as a reference, scaled and presented as a Hounsfield or CT number (HU) which is defined as:

$$HU = 1000 \frac{\mu_m - \mu_{\text{water}}}{\mu_{\text{water}}}$$

Where,  $\mu_m$  and  $\mu_{\text{water}}$  are the linear attenuation coefficients for the tissue material and for water, respectively. The CT- number of water is therefore zero. CT numbers for a variety of tissues are shown in the following table(11).

*Table 2. 1 CT number of various tissues*

Tissue	CT number (HU)
Lung	-300
Fat	-90
White Matter	30
Gray Matter	40
Muscle	50
Trabecular Bone	300-500
Cortical Bone	600-3000

CT can generate a patient specific attenuation map for correcting the radionuclide image for photon attenuation. In a clinical setting, this can be performed by scanning the patient in the CT scanner and then moving the patient to a SPECT system for acquisition of the radionuclide data. A challenging problem occurs because the x rays and radionuclide data must be registered spatially with the CT derived attenuation map for reconstruction. However, the linear attenuation coefficient measured with CT is calculated at the x ray energy rather than at the energy of the photon emitted by the radiopharmaceutical acquired during the radionuclide imaging study. It is therefore necessary to convert the linear attenuation coefficients obtained from the CT scan to those corresponding to the energy of the emission photons used for the radionuclide imaging study. The SPECT/CT systems have been developed similar methods for calibration the CT image for attenuation correction of the emission data(11).

#### 2.1.4 Partial volume effect (PVE)

When the size of the objects is less than approximately three times the resolution of the system result in lower concentrations of radioactivity (MBq/cc) in the region of interest than the actual value (Hoffman et al 1979).The partial



volume effect refers to both under/overestimation of activities around small structures in the reconstruction image. This phenomenon has usually occurred due to the relatively low image resolution of the SPECT system and the limited image sampling (Soret et al., 2007). The Recovery coefficient (RC) value is the ratio between the reconstructed count activity and true count activity of region of interest and should be 1 for larger object. Recovery coefficient is applied for correcting the over/underestimation of activities from partial volume effect in a small structure. This coefficient can be determined by measuring the activity concentration within different object sizes. The example of the RC curve is illustrated as in figure 2.1(3).

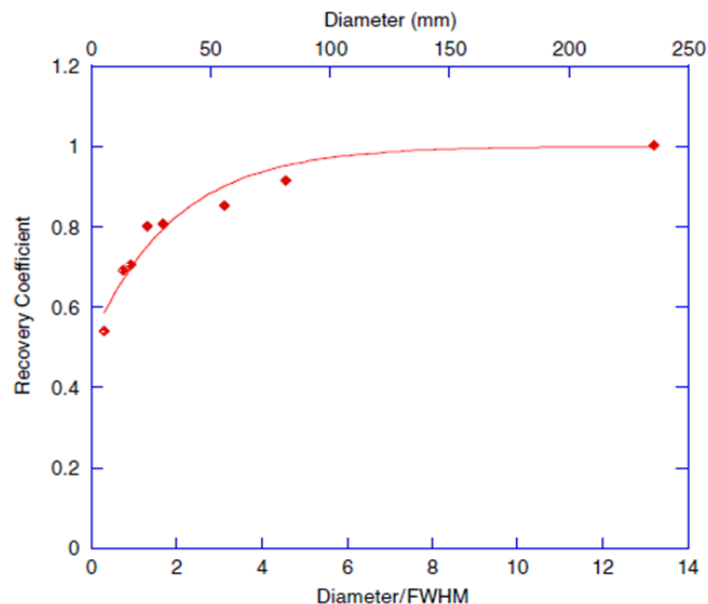


*Figure 2. 1 The plot of recovery coefficient values against object diameter as a fraction of the system spatial resolution, represented as the FWHM (mm). (Willowson, K., et al(3))*

## 2.2 SPECT reconstruction

Methods of image reconstruction using the acquired data fall into two categories: iterative methods and analytic methods. Analytic methods are based on exact mathematical solution to the image reconstruction problem, whereas iterative methods estimate the distribution through successive approximations. Accurate

correction for attenuation and their degradations require more complex iterative reconstruction techniques.

### 2.2.1 Iterative reconstruction

Iterative reconstruction technique requires many more calculations and much more computed time to create a trans-axial image than does FBP. It is a method of algorithms used to reconstruct 2D and 3D images from the projections of an object. There are a large variety of algorithms, but each starts with an assumed image, computes projections from the image, compares the original projection data and updates the images based upon the difference between the calculated and the actual projections. Although conceptually this approach is much simpler than filter back-projection, for medical applications, it has traditionally lacked the speed of implementation and accuracy. This is due to the slow convergence of the algorithm and high computational demands. The major advantages of the iterative approach include in sensitivity to noise and the capability of reconstructing an optimal image in the case of incomplete data. Situations where it is not possible to measure all 180 degrees may be more amenable to solution by this approach. The method has been applied in emission tomography modalities like SPECT and PET. The type of iterative reconstruction currently uses is the ordered subset expectation maximization (OSEM) method, in which the projection data are ordered into subsets, which are used in the iterative steps of the reconstruction to speed up the process. The advantage of OSEM is that an order of magnitude increase in computational speed can be obtained (12).

### 2.2.2 Quantitative Analysis

Quantitative methods have been used to measure cardiac function as well as regional cardiac function from SPECT images during the past of 10 years. This is because the pixel count value from within the cardiac region is related to some parameter of cardiac performance (13). In the case of myocardial perfusion imaging, the pixel count value of the region is related to the concentration of radionuclide and blood flow. Two standard types of quantification are: absolute

quantification, which is the ability to extract from a pixel number of counts from giving radionuclide concentrations at the source locations and the true relative quantification, which is able to extract from pixels the ratio of the counts expected from a given ratio for radionuclide concentrations at two source locations. In the present, the most widely used approach is using data based methods of quantification. The concept of data based quantification involved three major steps:

1. To enhance the image in term of image processing(14).
2. To extract pertinent measurement to use in determining normality versus abnormality in term of Image analysis
3. To qualify the degree of abnormality by comparing the extracted measurement to normal database.

Many of the techniques illustrate reflect computer method developed at Cedars-Sinai Medical Center. The Cedars-Sinai quantitative approach to SPECT is based on sampling the patient's short and vertical long axis myocardial tomogram using maximum count circumferential profiles and comparing this profile to profile derived from a database of normal patients. Patient profile points that fall below the normal limit and meet a criterion for abnormality are considered abnormal. The quantitative output of the program includes a polar map display design being abnormality and a report indicating the percent of abnormal pixel within the total and individual vascular territories. QPS provides three perfusion polar maps and three 3D parametric surfaces (stress, rest and reversibility). The function pull-down menu contains the options "Raw", "Severity", and "Extent", all of which apply to both 2D and 3D displays.

### 2.2.3 SPECT/CT

The advantage of combining SPECT with CT is numerous and is primarily due to the anatomic referencing and the attenuation correction capabilities of CT. A SPECT/CT scanner is an integrated device containing both a CT scanner and a SPECT camera and therefore capable of obtaining a CT scan, a SPECT scan, or both. Combined SPECT/CT imaging provides sequentially functional information

from SPECT and the anatomical information from CT, obtained during a single examination. CT data are also used for rapid and optimal attenuation correction of the single photon emission data and precise location of abnormal area and physiological tracer uptake. SPECT/CT improves sensitivity and specificity, but can also aid in achieving accurate dosimetry estimates as well as in guiding Interventional procedure or in better defining the target volume for external beam radiation therapy. (11)

The development of instruments, computer-based procedures for image analysis and display, new radioisotope labelled agents for visualization of biologically significant events enhance the SPECT/CT in term of clinical impact on patients care and cost effectiveness. SPECT/CT data also provide a better region of interest definition for quantification of radiopharmaceutical uptake in a lesion. SPECT/CT registration is the process of aligning SPECT and CT images for the purposes of combined image display and image analysis. SPECT/CT fusion is the combined display of registered SPECT and CT image sets. Superimposed data typically are displayed with the SPECT data color coded in the CT data in gray scale. (17)

### 2.3 Review of related literatures

Bailey, D L., Willowson, K P., et al (3) reported an article on an evidence-based review of quantitative SPECT imaging and potential clinical applications. They review the current status of SPECT imaging and clinical applications for quantitative interpretations, consider the requirements for quantitative SPECT imaging instrumentation, software, and image calibration and acquire knowledge of the capabilities of quantitative SPECT with a view to developing new clinical applications.

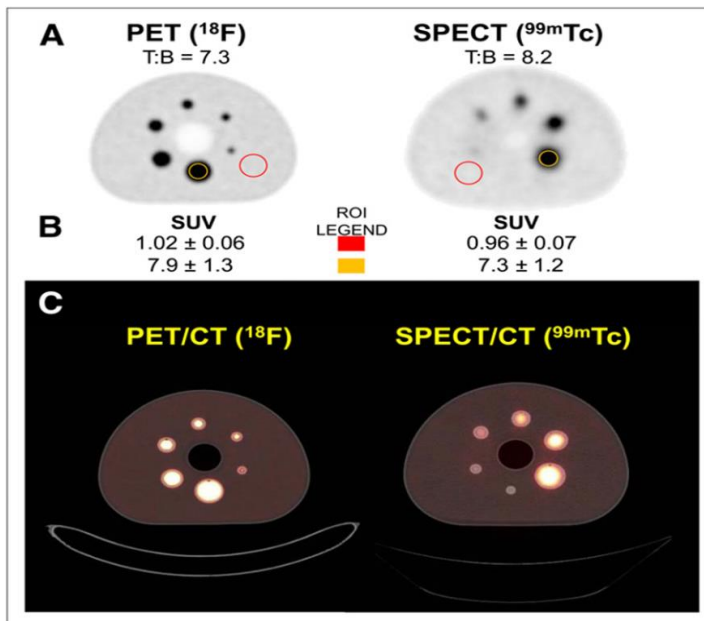


Figure 2. 2 Comparison of quantitative PET ( $^{18}\text{F}$ ) and SPECT ( $^{99\text{m}}\text{Tc}$ ) images in IEC phantom.

The requirements for producing quantitative data in emission tomography are the same for PET and SPECT. The main features are a reconstruction algorithm that behaves in a linear fashion in terms of the reconstructed radioactivity concentration, an algorithm to compensate for photon absorption within the body, an algorithm to remove scattered radiation from the data, and the ability to calibrate the reconstructed data in  $\text{kBq}/\text{cm}^3$ .

Table 2.2 Impact on recovered SUV is more significant in SPECT than in PET, as SPECT systems have poorer spatial resolution. Both systems significantly underestimate SUV for sphere diameters of less than approximately 3 times the respective system spatial resolution.

*Table 2. 2 SUVs for compartments of IEC phantom for SPECT and PET*

Sphere diameter (mm)	SPECT SUV (8.2)	Difference	PET SUV (7.3)	Difference
Background (SUV = 1)	0.96	-4.0%	1.02	+2.0%
37	7.3	-11.0%	7.9	+7.6%
28	6.5	-21.3%	7.7	+5.3%
22	4.5	-44.8%	7.6	+3.5%
17	3.2	-60.6%	7.1	-3.0%
13	2.9	-64.6%	6.2	-14.9%
10	2.9	-65.2%	4.1	-43.7%

Although SPECT is a widely used clinical imaging modality, it will not achieve its full potential when it is used in a purely qualitative manner. The combined SPECT/CT is a game-changer in numerous ways and provides the effectiveness for a shift in SPECT use into the quantitative domain in radionuclide emission tomography. The users should be aware of the deterioration in quantitative accuracy with decreasing object size when objects below 3 times the spatial resolution of the system are imaged.

Da Silva AJ et al (5) reported an article on the absolute Quantification of Regional Myocardial Uptake of  $^{99m}\text{Tc}$ -Sestamibi with SPECT. In these experiments, in vivo measurements of the radionuclide uptake in the myocardium was compared directly with ex vivo activity concentration measurements of the excised tissue. By correcting for both attenuation and partial-volume errors, they were able to achieve absolute quantification with an accuracy error near 10%.

## True activity Vs Measured activity

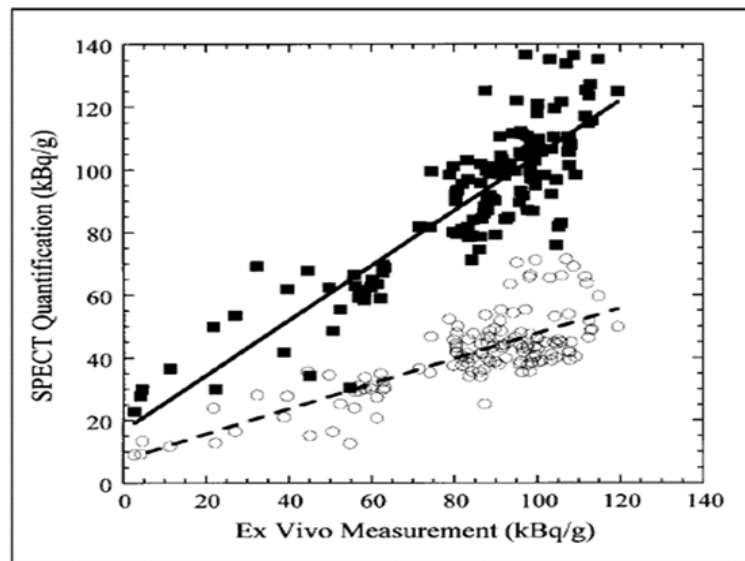


Figure 2. 3 SPECT quantification obtained from postmortem images vs. ex vivo activity concentration for eight pigs included in study.  $\circ$ =activity concentration measured in every myocardial segment with only attenuation correction applied.  $\blacksquare$  = activity concentration measured in every myocardial segment with both attenuation and partial-volume corrections applied(5).

In this research, they describe a new technique for quantifying myocardial SPECT images that accounts for attenuation and partial volume correction using co-registered CT images. The CT image provides both an object-specific attenuation map for SPECT reconstruction and an anatomic template to define the regions of interest for quantification of the SPECT image. The effectiveness of this technique showed in animal experiments had been able to measure the absolute regional radionuclide content in porcine myocardium in vivo(5)

The effectiveness of these methods as mentioned above, this research planned to evaluate the absolute quantitative measurement based upon partial volume correction and attenuation correction derived from x-ray computed tomography using phantoms and patient's data of myocardial perfusion imaging.

## CHAPTER III

### RESEARCH METHODOLOGY

#### 3.1 Research design

This study is an experimental descriptive study. The steps of the procedure are shown as the following figure 3.1. (15)

#### 3.2 Research design model

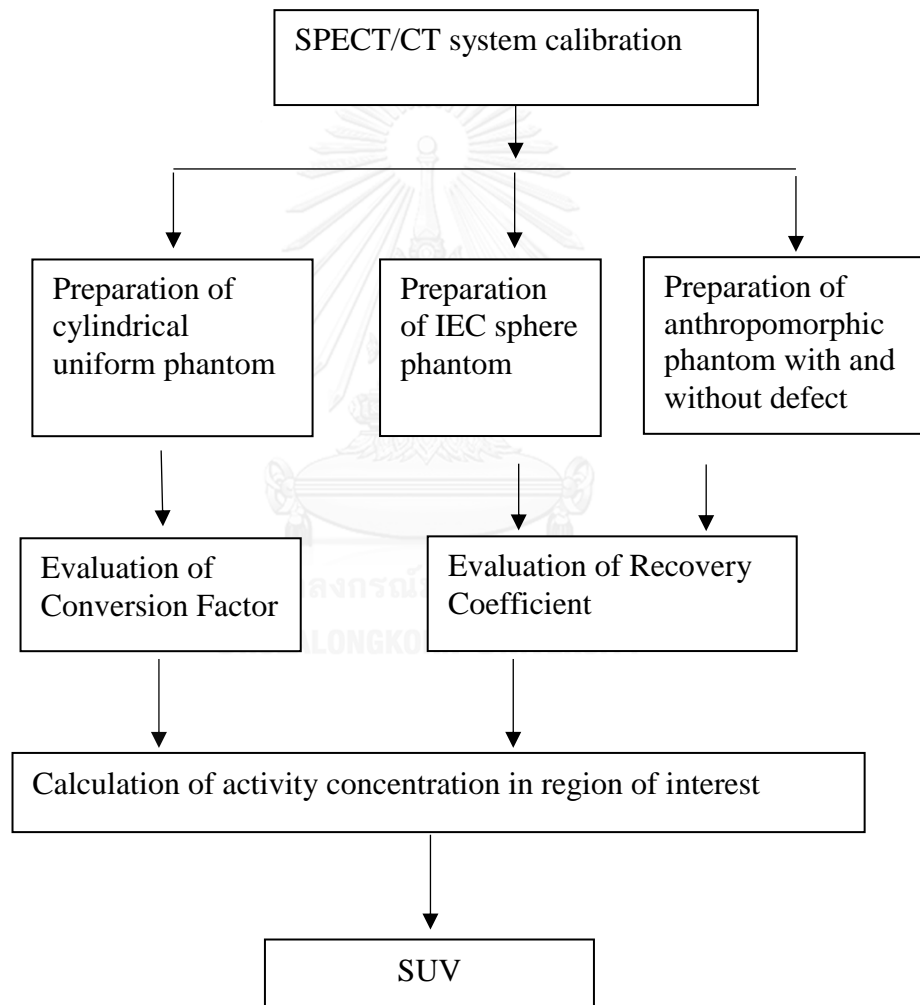


*Figure 3. 1 Research design model*



### 3.3 Conceptual framework

Three factors influencing the accuracy of Standardized Uptake Value (SUV) of the myocardial perfusion images are the injected activity, the patient body weight and the activity concentration of region of interest. Those could be corrected by applying the conversion factor and recovery coefficient to the SUV. The conceptual framework of this study is shown in figure 3.2.

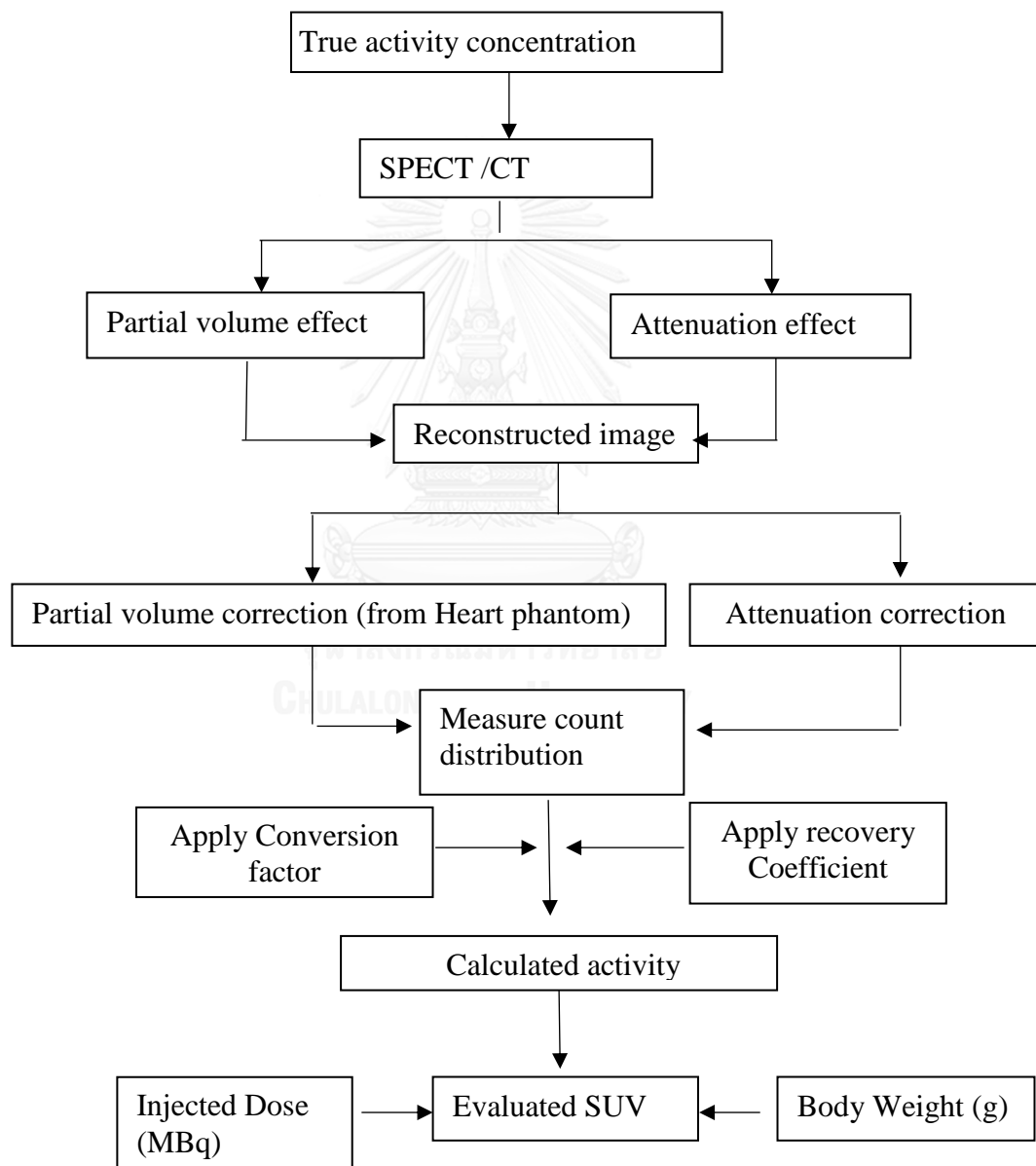


Figure 3. 2 Conceptual framework

### 3.4 Research question

#### 3.4.1 Primary research question

What is the best method to calculate the Standardized Uptake Value in myocardial perfusion SPECT/CT?

#### 3.4.2 Secondary research question

What are conversion factor and recovery coefficient?

### 3.5 Key words

SPECT/CT

STANDARDIZED UPTAKE VALUE

QUANTITATIVE STUDY

MYOCARDIAL PERFUSION

<sup>99m</sup>Tc- SESTAMIBI

### 3.6 The sample

The conversion factor was determined by acquiring the tomographic cylindrical uniform phantom filled with technetium-99m solution of recorded activity and time at three different times. The recovery coefficient was determined by acquiring tomographic anthropomorphic thorax phantom filled with technetium-99m in heart and body of known concentration at three different times. The SUVs were studied in phantom and in 20 normal myocardial perfusion patients of 10 male and 10 female. The number of the abnormal patients sample is determined by the following formula:

$$N = \frac{Z_{\alpha/2}^2 P (1-P)}{d^2} = 25.008$$

Where, N= Sample size

Z=95% , Confidence Interval =1. 96

P=Proportion of abnormal=7% = 0.07 (Da Silva, A J., Tang, H R., et al, JNM- 2001)

d=Acceptable error=10% = 0.1

### 3.7 Materials

#### 3.7.1 Single Photon Emission Computed Tomography/ Computed Tomography (SPECT/CT)

The SPECT/CT system model Symbia T6 manufactured by Siemens Medical Solution as shown in figure 3.3 was installed in 2009 at Division of Nuclear Medicine, King Chulalongkorn Memorial Hospital, Bangkok. The system integrates a SPECT scan with six-multi slice CT scans using Syngo multimodality computer platform. Dual SPECT detector of NaI (Tl) crystal is 59.1x44.5 cm, field of view is 53.3x38.7 cm and the total number of photomultiplier tubes is 59. CT scan collects the data simultaneously via a 6- row detector. The maximum FOV is 50 cm, the gantry - bore diameter is 70 cm. Three kVp settings are available at 80, 110 and 130 kVp. The tube current ranges from 20 to 345 mA.



*Figure 3. 3 SPECT/CT system*

#### 3.7.2 Cylindrical uniform phantom

The phantom is made of a hollow plastic cylinder with the inner volume of 6,293 cc. The phantom is filled with  $^{99m}\text{TcO}_4^-$  solution of uniformly distribution as in figure 3.4.



*Figure 3. 4 Cylindrical uniform phantom*

### 3.7.3 Anthropomorphic thorax and heart phantom

Anthropomorphic thorax and heart phantom, as in figure 3.5, includes liver, lungs, heart and spine inserts. Lung inserts filled with Styrofoam beads and water to simulate lung tissue density. The cardiac insert dimension is chamber length 8.6 cm, diameter 6 cm, myocardial volume 118 cc, ventricular volume 60 cc and thickness 9.5 mm. The volumes are left lung 900 cc, right lung 1100 cc, liver 1,200 cc and background 10,300 cc.

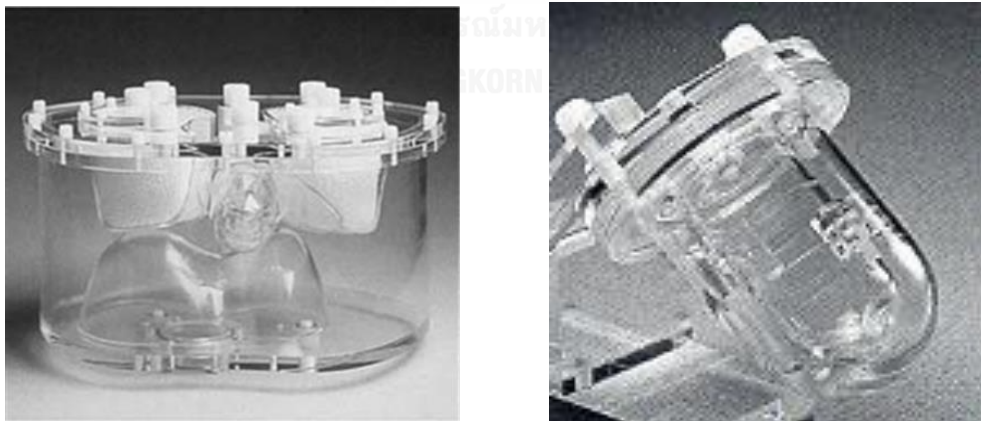


*Figure 3. 5 Anthropomorphic thorax and heart phantom (left) myocardial chamber (right)*

### 3.7.4 Torso phantom with hollow sphere inserts (IEC)

The torso phantom with dimension of 24.1 x 30.5 x 24.1 cm (height x width x depth) consists of six hollow sphere inserts with inner diameters of 1.0, 1.3, 1.7, 2.2, 2.8 and 3.7 cm, and the wall thickness of 1 mm (figure 3.6). The volume of the torso phantom is 9,700 cc and the six spheres are 0.52, 1.15, 2.57, 5.58, 11.50 and 26.63 cc, respectively



*Figure 3. 6 Torso phantom with six hollow sphere inserts*

### 3.7.5 Technetium pertechnetate ( $^{99m}\text{TcO}_4^-$ )

Technetium is obtained from a generator in normal saline solution (0.9% NaCl) as the pertechnetate ion,  $^{99m}\text{TcO}_4^-$ . Technetium-99m is a metastable nuclear isomer of technetium-99, symbolized as  $^{99m}\text{Tc}$ . The “m” indicates a metastable nuclear isomer; its half-life is considerably longer than most nuclear isomers, which undergo gamma decay.

Technetium-99m is used as a radioactive tracer detected in the body. It is well suited to the role because it emits readily detectable 140 keV gamma rays and its half-life for gamma emission is 6.0058 hours. The short half-life of the isotope allows for scanning procedure, collect data rapidly but keep total patient radiation exposure low. In the myocardial perfusion scan,  $^{99m}\text{Tc}$ -sestamibi is used. Scanning is performed with SPECT/CT. In a phantom study,  $^{99m}\text{TcO}_4^-$  is used because of low cost and the mechanism is similar to  $^{99m}\text{Tc}$ -sestamibi.

## 3.8 Methods

This study is carried out as the following:

### 3.8.1 SPECT/CT daily QC [APPENDIX C]

The daily quality control program for CT is performed using water phantom for the study of image quality, kVp calibration, pixel noise and CT number values. For SPECT system, the flood-field uniformity is evaluated intrinsically for the response of the detector operation. Uniformity is measured daily over the useful field of view and central field of view. The COR must be accurately aligned with the center of the acquisition matrix in the computer, frequency of test is weekly.

### 3.8.2 The preparation of cylindrical uniform phantom

The phantom contains 650 MBq of  $^{99m}\text{Tc}$  solution of uniformly distribution. The activity concentration of the  $^{99m}\text{Tc}$  is 0.103 MBq/cc. The acquisition protocol is 32 views for 60 seconds per view over 180-degree arc. Standard protocols of emission scan of step and shoot, 3 degrees per step, matrix size 128x128, and zoom factor 1 are used. For CT scan, the parameters are tube voltage kVp 130, slice width 5 mm, pitch factor 0.6 and FOV 500 mm. The acquisition time for SPECT scan is 30 minutes. An iterative reconstruction is applied with attenuation correction by order 4 and subsets 15 with OSEM flash 3 D.

### 3.8.3 The preparation of anthropomorphic thorax and heart phantom

The myocardial wall is filled with  $^{99m}\text{Tc}$  activity concentration of 0.132MBq/cc. The ventricle chamber is filled with Tc-99m activity concentration of 0.01MBq/cc the same as the background activity concentration with the total volume of 10,300 cc. The inserted lung is not filled  $^{99m}\text{Tc}$  and liver filled the same activity concentration as the background.

The myocardial wall with defect is filled with different activity concentration of Tc-99m. The defect size ( $90^\circ$ , 2 cm (h), 10 mm (thick) / Vol ~ 5.4 ml) is placed at antero-lateral wall of the myocardium. The activity concentration filled into the

inserted myocardial defect varied into 0%, 25%, 50% and 75% of the normal myocardial wall.

The acquisition protocol consists of 32 views, 30 seconds per view over 180-degree arc. The simplest automatic contour consists of approximating the object outline by an ellipse drawn around the edges of the object. Uniform attenuation is then assigned within the contour to generate the attenuation map. Standard protocols of emission scan of step and shoot, 3 degrees per step, matrix size 64x64, and zoom factor 1.45 are used. For CT scan, the parameters are tube voltage 130 kVp, slice width 5 mm, pitch factor 0.6 and FOV 500 mm. The acquisition time for SPECT scan is about 18 minutes. An iterative reconstruction is applied with attenuation correction by order 4 and subsets 15 with OSEM flash 3 D.

#### 3.8.4 The preparation of hollow sphere phantom

The spheres are filled with  $^{99m}\text{Tc}$  activity concentration of 0.058 MBq/cc. The solution is well mixed before filling into the spheres. The acquisition protocol consists of 32 views, 60 seconds per view over 180-degree arc. Standard protocols of emission scan of step and shoot, 3 degrees per step, matrix size 128x128, and zoom factor 1 are used. For CT scan, the parameters are tube voltage 130 kVp, slice width 5 mm, pitch factor 0.6 and FOV 500 mm. The acquisition time for SPECT scan is about 30 minutes. An iterative reconstruction is applied for attenuation correction by order 4 and subsets 15 with OSEM flash 3 D.

#### 3.8.5 Patient study

All patients underwent stress-rest  $^{99m}\text{Tc}$ -Tetrofosmin MPI protocol. For both stress and rest, SPECT images were acquired 45-60 min after tracer injection(16). The acquisition consists of low-energy, ultra high resolution collimators, 20% symmetrical window at 140 keV, matrix 64 x 64, zoom factor 1.45. A non-circular orbit with step and shoot acquisition at 3 degree intervals over a 180 degree arc extending from 45 degree right anterior oblique to 45 degree left posterior oblique with 32 views and

dwelling time of 50s per view were used. All patients were imaged in supine position with arms placed above the head. The acquisition time was 26 minutes for the stress images and the rest images. CT scan was acquired with 130 kVp and 20 mAs with 5-mm slice thickness. SPECT reconstruction was performed using Flash 3D OSEM.

### 3.8.6 Data analysis

#### 3.8.6.1 Conversion Factor (CF)

The conversion factor is calculated by the following equation.

$$CF = \frac{\text{Measured count concentration from reconstructed image}}{\text{Activity concentration in solution}}$$

$$\text{Activity concentration in solution} = \frac{\text{True activity concentration (MBq)}}{\text{Phantom volume (cc)}}$$

Measured count concentration is calculated by using the VOI tool on the reconstructed image. The unit of Conversion Factor is (counts/minute/activity).

#### 3.8.6.2 Recovery coefficient

The recovery coefficient is calculated by the following equation.

For IEC sphere phantom,

$$\text{Recovery coefficient} = \frac{\text{Apparent concentration in sphere}}{\text{True concentration in sphere}}$$

For heart and thorax phantom,

$$\text{Recovery coefficient} = \frac{\text{Apparent concentration in cardiac chamber}}{\text{True concentration in chamber}}$$

A recovery coefficient is used to correct the partial volume effect for the underestimated concentrations of small object which is measured from reconstructed images.



### 3.8.6.3 Standardized Uptake Value

The conversion factor and recovery coefficient are applied to the anthropomorphic phantom with the defect and the patients underwent  $^{99m}\text{Tc}$ -Sestamibi SPECT/CT for myocardial perfusion study.

Standardized Uptake Value is calculated by the following equation.

$$\text{SUV} = \frac{\text{Activity concentration in VOI (MBq/cc)}}{\text{Injected dose (MBq)/Body weight(g)}}$$

### 3.9 Statistical analysis

Body weight and injected dose are collected from PACS system. Data are expressed as mean  $\pm$  SD of SUV. Stress and rest SUV by e-soft auto contour method are compared by using pair t- test. p value of less than 0.05 is considered statistically significant. To detect abnormality, z scoring method (mean SUV<sub>pt</sub> – mean SUV<sub>normal</sub>)/SD is used.

### 3.10 Ethical Consideration

This study is designed to test both in-vitro and in-vivo studies. Cylindrical uniform phantom, hollow sphere phantom, anthropomorphic thorax and heart phantom are included in vitro study. In-vivo study is not directly tested in patients, the myocardial perfusion images are used in order to achieve standardized uptake value. The ethical is approved by the Ethics Committee of Faculty of Medicine, Chulalongkorn University.

### 3.11 Expected benefits

The Standardized Uptake Values of myocardial perfusion scan for normal and abnormal Thai patient are obtained. The factors affecting activity concentration are obtained.

## CHAPTER IV

### RESULTS

#### 4.1 The conversion factor (CF)

The true activity concentration of  $^{99m}\text{Tc}$  for the first, second and third scans using cylindrical uniformity phantom were 0.0746 MBq/cc, 0.0690 MBq/cc, 0.0646 MBq/cc respectively. The acquisition time for each scan is 30 minutes. The results and images of CF for three scans are shown in table 4.1 and figure 4.1.

*Table 4. 1 The conversion factors (CPM/MBq) from 3 acquisitions*

No. of acquisition	Total counts	Volume (cc)	Counts/cc	CPM /cc	CF (CPM/MBq)
1	66721240	6119.9	10902.34	363.41	4871.47
2	61698976	6097.63	10118.52	337.28	4888.17
3	57340240	6087.93	9418.68	313.96	4867.53
				Average CF	4875.72

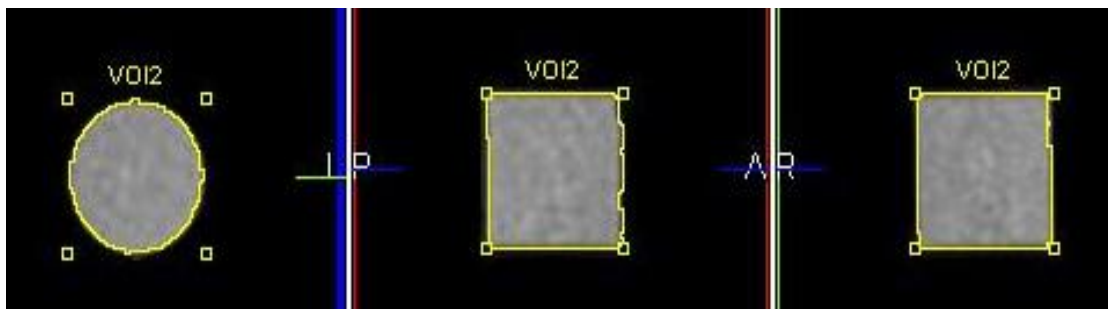


*Figure 4. 1. The reconstructed image of cylinder uniformity phantom, Left image is transverse axial, middle image is sagittal and right image is coronal image.*

## 4.2 The recovery coefficient (RC)

### 4.2.1 The RC of the anthropomorphic phantom with six sphere inserts

The validation of the recovery coefficient from the anthropomorphic with hollow sphere inserts is described first. The true activity concentration of  $^{99m}\text{Tc}$  for first, second and third acquisition scan were 0.056MBq/cc, 0.053MBq/cc, 0.048MBq/cc respectively. The acquisition time for each scan was 30 minutes. The conversion factor 4875 CPM/MBq was applied to convert counts to activity concentration. The results of three acquisition scans are shown in Table 4.2. Figure 4.2 shows the reconstructed image of IEC phantom as the function of 6 sphere volumes.

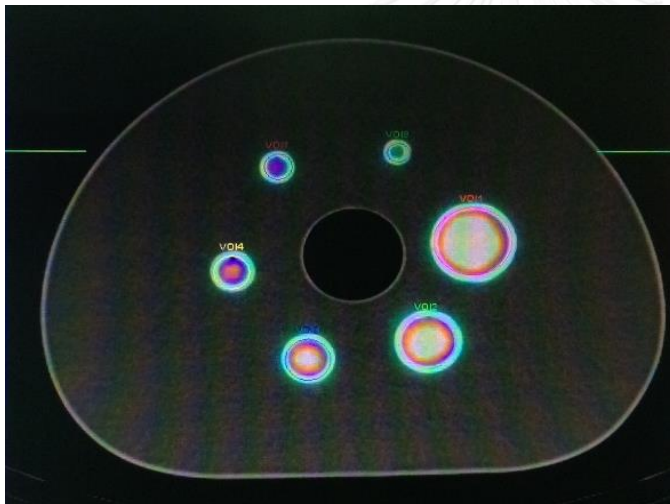


*Figure 4. 2 Reconstructed image of the IEC phantom with six sphere inserts filled with Tc-99m solution.*

*Table 4. 2 The value of the recovery coefficient of six spheres*

	Sphere volume (cc)	Total counts	Counts/cc	CPM/cc	Act conc: MBq/cc	RC
Scan no.1	26.57	136563	5139.74	171.32	0.035	0.628
	11.57	51420	4444.25	148.14	0.030	0.543
	5.64	23264	4124.82	137.49	0.028	0.504
	2.62	9682	3695.42	123.18	0.025	0.452
	1.18	3456	2928.81	97.63	0.020	0.358
	0.55	912	1658.18	55.27	0.011	0.203
Scan no.2	26.83	131867	4914.91	163.83	0.034	0.649
	11.72	50266	4288.91	142.96	0.029	0.566
	5.64	22478	3985.46	132.85	0.027	0.526
	2.62	8108	3094.66	103.16	0.021	0.408
	1.18	2802	2374.58	79.15	0.016	0.313
	0.54	670	1240.74	41.36	0.008	0.164
Scan no. 3	26.83	115710	4312.71	143.76	0.029	0.609
	11.56	46155	3992.65	133.09	0.027	0.564
	5.64	19463	3450.89	115.03	0.024	0.488
	2.62	8065	3078.24	102.61	0.021	0.435
	1.18	2758	2337.29	77.91	0.016	0.330
	0.54	784	1451.85	48.39	0.010	0.205

*Table 4. 3 The average value of recovery coefficient*

Sphere Volume (cc)	Recovery coefficient
26.743	0.629
11.617	0.558
5.640	0.506
2.620	0.432
1.180	0.334
0.543	0.191

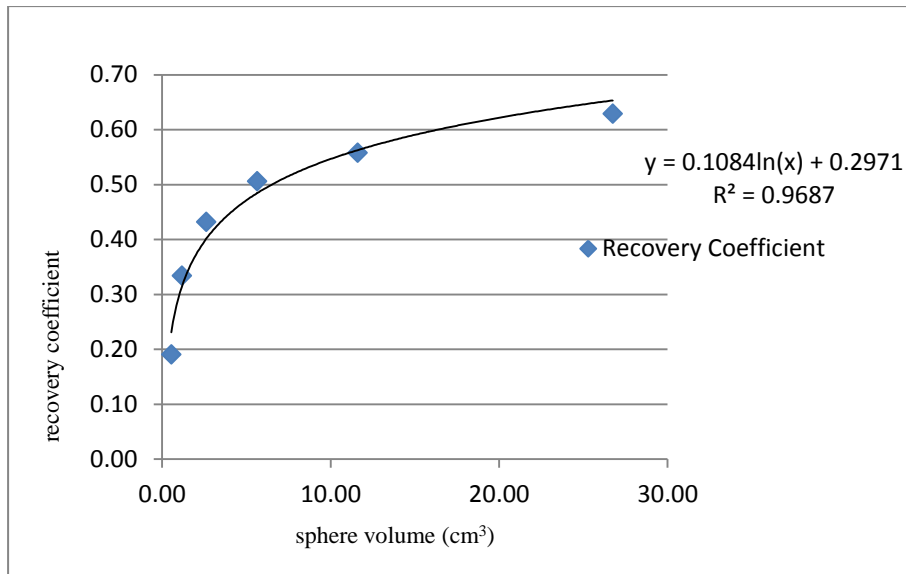


Figure 4. 3 Sphere volume vs recovery coefficient

#### 4.2.2 The RC of anthropomorphic heart and thorax phantom

The anthropomorphic heart and thorax phantom without defect is used to determine the recovery coefficient, which will be applied to the patient data. The true activity concentration of  $^{99m}\text{Tc}$  in myocardium for three scans is 0.132MBq/cc, 0.125MBq/cc, 0.118 MBq/cc. The results are shown in table 4.4. The acquisition time for each scan was 17.4 minutes. The myocardial wall thickness is 9.5 mm.

Table 4. 4 . The recovery coefficients of the anthropomorphic thorax phantom

Acquisition no.	Total counts	Cardiac wall Volume(cc)	Counts /cc	CPM/cc	Act conc: (MBq/cc)	Recovery coefficient
1	754178	118	6391.34	367.32	0.075	0.571
2	695668	118	5895.49	338.82	0.070	0.558
3	667485	118	5656.65	325.09	0.067	0.567
Average recovery coefficient						0.565

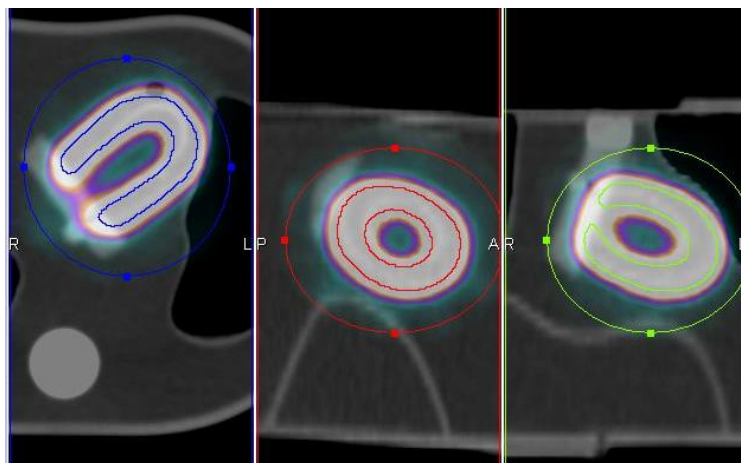
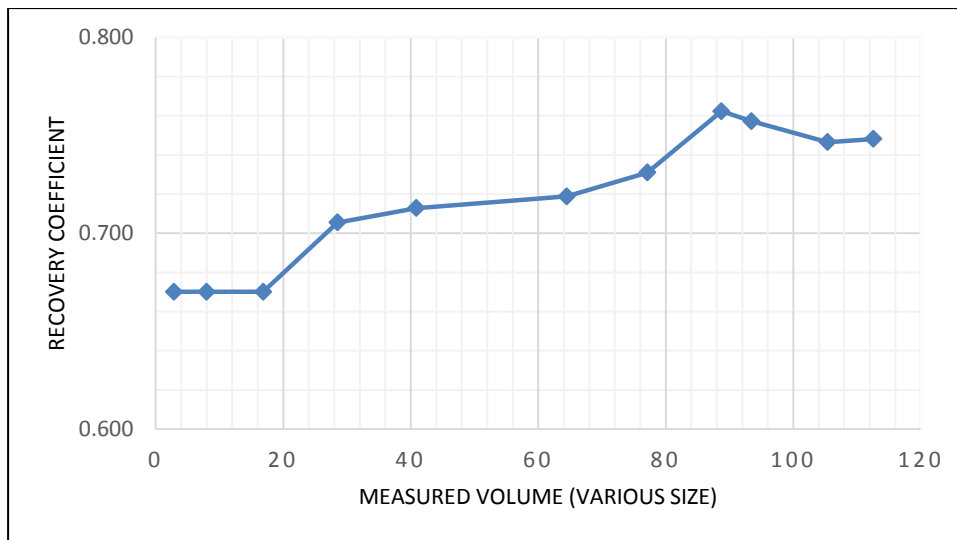


Figure 4. 4 The reconstructed images of myocardial phantom, Left image is transverse axial, middle image is sagittal and right image is coronal image.

New recovery coefficients are recorded by drawing volume of interest in various size on the normal myocardium with 3 D iso-contour method. The data and the graph are shown in table 4.5 and figure 4.5, respectively.

Table 4. 5. The recovery coefficients of the anthropomorphic thorax phantom

Total counts	Volume (cm <sup>3</sup> )	Count/cc	Count/min /cc	Activity Conc: (MBq/cc)	Recovery Coefficient
19252	2.88	6684.7	384.2	0.079	0.670
53094	7.98	6653.4	382.4	0.078	0.670
111485	16.88	6604.6	379.6	0.078	0.670
200645	28.51	7037.7	404.5	0.083	0.706
290848	40.9	7111.2	408.7	0.084	0.713
462488	64.5	7170.4	412.1	0.085	0.719
562430	77.13	7292.0	419.1	0.086	0.731
674865	88.75	7604.1	437.0	0.090	0.762
705743	93.43	7553.7	434.1	0.089	0.757
784896	105.4	7446.8	428.0	0.088	0.747
840382	112.6	7463.4	428.9	0.088	0.748



*Figure 4. 5 Measured volume versus Recovery Coefficient*

### 4.3 Anthropomorphic Heart and Thorax Phantom with 5 cc defect

The inserted myocardial defects were filled with 4 different concentrations i.e. 0% (no activity), 25%, 50% and 75% of the outer normal myocardial wall concentration. For 0% defect, the true activity concentration of outer myocardial wall was 0.163 MBq/cc. For 25% defect, the defect concentration and outer myocardial wall concentration were 0.036 MBq/cc and 0.143 MBq/cc respectively. For 50 % defect, the defect concentration and the outer myocardial wall concentration were 0.072 MBq/cc and 0.144 MBq/cc respectively. For 75% defect, the defect concentration and the outer myocardial wall concentration were 0.117 MBq/cc and 0.155 MBq/cc respectively. The acquisition time for each scan was 17.4 minutes.

Percent defect was measured by using the following formula.

$$\text{Percent defect} = 100 \times \frac{\text{Defect activity concentration/ Recovery Coefficient}}{\text{Normal myocardium activity conc./Recovery Coefficient}}$$

The conversion factor of 4875 counts per minute per MBq which is calculated from cylindrical uniform phantom study, the recovery coefficient value is 0.565 which is calculated from anthropomorphic heart and thorax phantom without defect study were applied. The correlation between true activity concentration and measured activity concentration before and after application of conversion factor and

recovery coefficient are shown in Table 4.6. The same size of region of interest and same recovery coefficient for defect and normal myocardium are used in this study.

*Table 4. 6 The relation between relative true activity concentration and measured activity concentration of percent defect.*

Method	Site	Act: Conc:	% defect	Act: Conc:	% defect	Act: Conc:	% defect	Act: Conc:	% defect
True Act:	Defect	0	0%	0.036	25%	0.072	50%	0.117	75%
	Normal	0.163		0.143		0.144		0.155	
Before correction with Recovery Coefficient									
Max: cts	Defect	0.00077	16.32%	0.00166	28.09%	0.0019	39.03%	0.00263	50.31%
	Normal	0.00477		0.00591		0.00486		0.00523	
Total cts	Defect	0.01274	21.16%	0.02267	28.75%	0.02845	39.32%	0.04377	54.61%
	Normal	0.06023		0.07886		0.07237		0.0816	
After correction with Recovery Coefficient									
Max: cts	Defect	0.00137	16.32%	0.00294	28.09%	0.00336	39.03%	0.00465	50.31%
	Normal	0.00844		0.01047		0.00861		0.00925	
Total cts	Defect	0.02255	21.16%	0.04013	28.75%	0.05037	39.32%	0.07748	54.61%
	normal	0.10659		0.13959		0.12810		0.14189	

The result of percent defect before correction and after correction with recovery coefficient are the same.



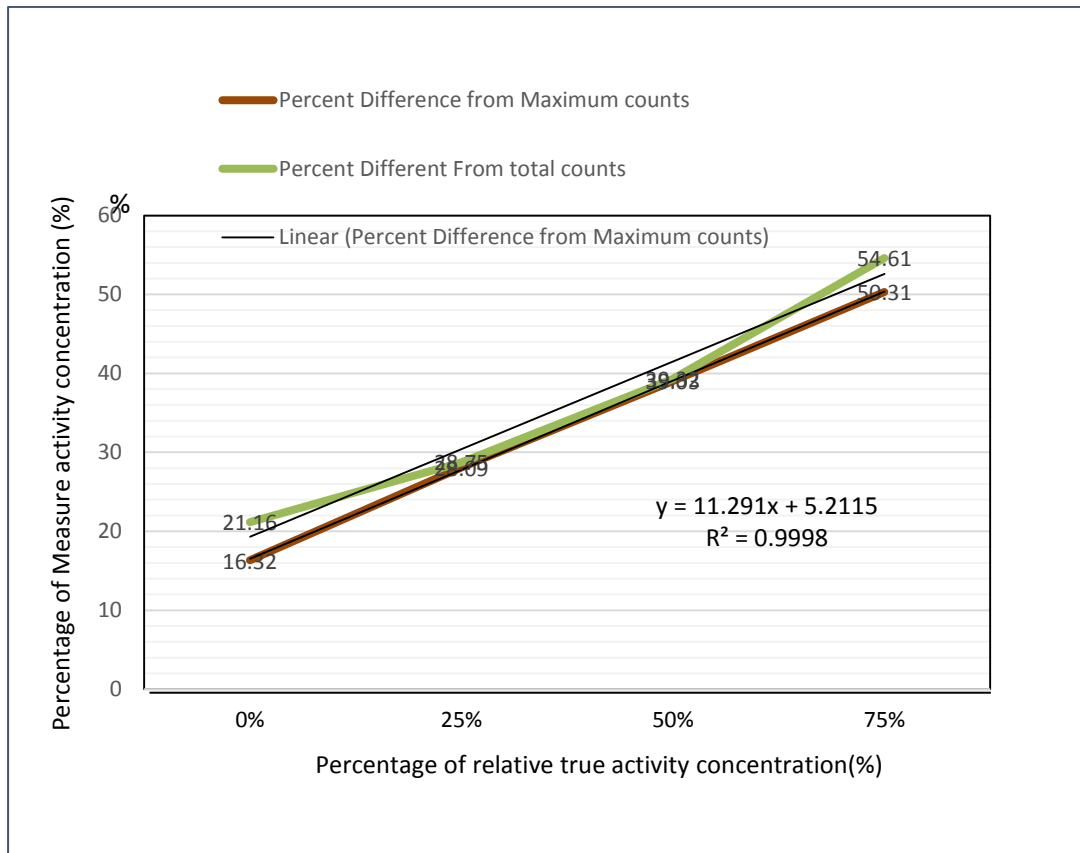


Figure 4.5 Measured percentage of defect in heart phantom before and after recovery coefficient application.

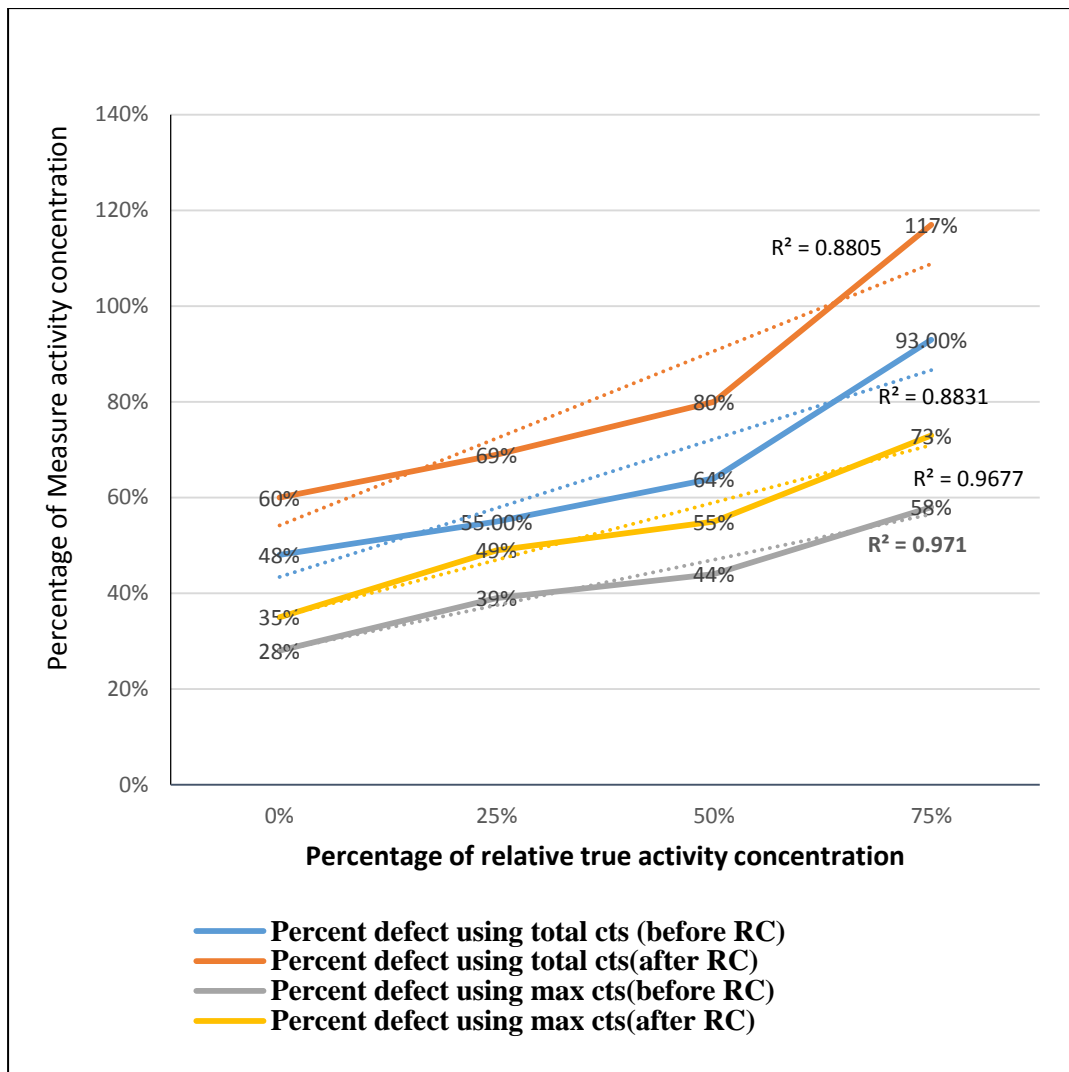
An alternative method of different region of interest is used in defect and normal myocardium. Recovery coefficient for defect is calculated from measured activity concentration of defect divided by true activity concentration of defect. Recovery coefficient of 0.451 is recorded for defect. Recovery coefficient of 0.565 which is recorded from heart and thorax phantom for normal myocardium. The relation between relative true activity concentration and measured activity concentration before and after different RC application by using maximum count and total count are shown in table 4.7, 4.8. The graph is shown in figure 4.6.

*Table 4. 7. The relation between relative true activity concentration and measured activity concentration of percent defect by applying different RC in AcC*

Percent defect using total counts								
Percent defect	avg	total	vol	cts/cc	cpm/cc	Act: conc	AcC (After RC)	
0%	defect	74.1	2225.0	1.64	1356.71	77.97	0.02	0.04
	normal	214.0	52220.0	18.40	2838.04	163.11	0.03	0.06
	Relative %						47.80	59.89
25%	defect	102.9	3293.0	1.65	1995.76	114.70	0.02	0.05
	normal	279.0	66506.0	18.33	3628.26	208.52	0.04	0.08
	Relative %						55.01	68.91
50%	defect	108.9	3485.0	1.67	2086.83	119.93	0.02	0.05
	normal	252.0	59142.0	18.12	3263.91	187.58	0.04	0.07
	Relative %						63.94	80.10
75%	defect	248.0	8434.0	1.86	4534.41	260.60	0.05	0.12
	normal	376.0	87293.0	17.94	4865.83	279.65	0.06	0.10
	Relative %						93.19	116.74
Percent defect using maximum counts								
0%	defect	214.9	74.1	3.8	56.553	3.250	0.001	0.001
	normal	770.0	214.0	3.8	202.632	11.645	0.002	0.004
	Relative %						27.909	34.964
25%	lesion	276.0	102.9	3.8	72.632	4.174	0.001	0.002
	normal	700.0	279.0	3.8	184.211	10.587	0.002	0.004
	Relative %						39.429	49.395
50%	defect	264.6	108.9	3.8	69.632	4.002	0.001	0.002
	normal	598.0	252.0	3.8	157.368	9.044	0.002	0.003
	Relative %						44.247	55.432
75%	defect	748.0	248.0	3.8	196.842	11.313	0.002	0.005
	normal	1292.0	376.0	3.8	340.000	19.540	0.004	0.007
	Relative %						57.895	72.529

*Table 4. 8. The relation between relative true activity concentration and measured activity concentration of percent difference by applying different RC in (%)*

TRUE	Percent defect using total cts (before RC)	Percent defect using total cts (after RC)	Percent defect using max cts (before RC)	Percent defect using max cts (after RC)
0%	48%	60%	28%	35%
25%	55%	69%	39%	49%
50%	64%	80%	44%	55%
75%	93%	117%	58%	73%



CHULALONGKORN UNIVERSITY

Figure 4. 6. Measured percentage of defect in heart phantom before and after recovery coefficient application with different RC

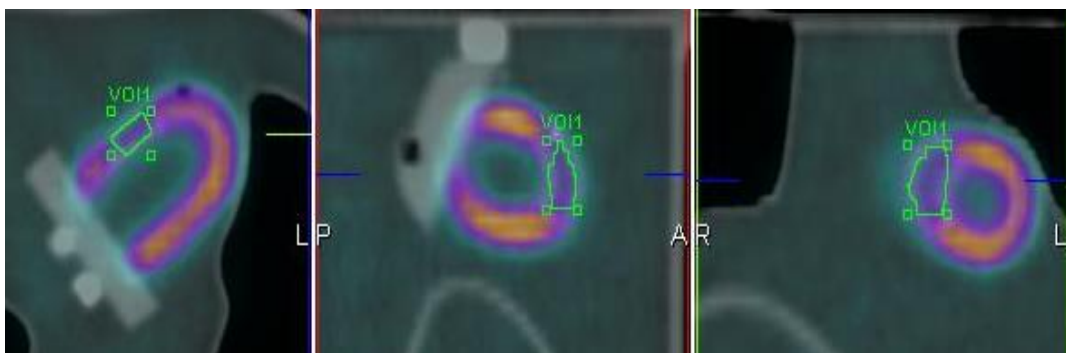
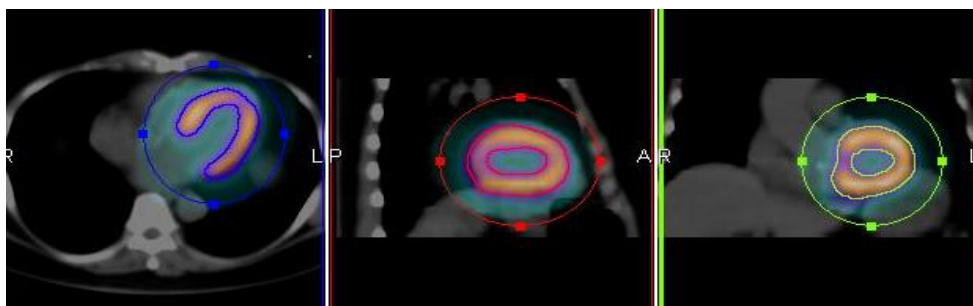


Figure 4. 7. Reconstructed images with 5 cc defect. Left image is transverse axial, middle image is sagittal and right image is coronal image.

#### 4.4 Standardized Uptake Value of normal myocardial perfusion scans

The overview of 10 male patients and 10 female patients who underwent the SPECT/CT imaging whose myocardial perfusion scan were normal are illustrated in table 4.9, 4.10, 4.11 and 4.12. The data analysis was carried out with two methods to determine the SUV (17). In the first method, the region of interest was drawn by e-soft auto ROI contour method with ISO 50% (Standard default from manufacturer). The volume of the left ventricular myocardium is measured by CT reconstructed images. Activity concentration is calculated from the counts in the region of interest which is then applied by the conversion factor 4875 CPM/MBq and recovery coefficient 0.565. Body weight and injected dose were recorded from patient's data. The example of normal myocardial perfusion reconstructed image is shown in fig 4.8.

In using the e-soft reconstruction algorithm, the mean and SD of Standardized Uptake Value of normal myocardial perfusion scan for rest and stress studies in all patients were  $8.15 \pm 1.21$  and  $8.00 \pm 1.5$  respectively. SUV for male and female were shown in table 4.9, 4.10, 4.11 and 4.12 separately. The comparison between rest and stress SUV in male and female studies were not significantly different ( $P > 0.05$ ). Using Image J software method, the average SUV for three vessels of the heart in normal myocardial perfusion imaging were  $7.70 \pm 1.2$  for LAD,  $8.13 \pm 1.1$  for LCX and  $7.61 \pm 1.3$  for RCA in rest scan and  $7.67 \pm 1.2$  for LAD,  $8.04 \pm 1.5$  for LCX and  $7.56 \pm 1.2$  for RCA in stress scan. The comparison between two methods were not significantly different ( $p = 0.28$ ).



*Figure 4. 8 Auto-contour ISO 50 % ROI for normal myocardial perfusion scan.*

*Table 4. 9 SUV for Rest normal myocardial perfusion scan in female patients*

Pat no.	Total counts	Volume (cc)	Counts /cc	CPM/cc	Act: Conc (MBq/cc)	RC apply Act: Con	Body Wt(g)	Inj dose (MBq)	SUV
1	1659071	129.50	12811.36	492.74	0.10	0.18	48200	903.82	9.54
2	1094703	142.00	7709.18	296.51	0.06	0.11	51900	749.86	7.45
3	1188386	144.60	8218.44	316.09	0.06	0.11	56100	725.73	8.87
4	1155492	149.00	7754.98	298.27	0.06	0.11	60000	909.96	7.14
5	1174114	126.40	9288.88	357.26	0.07	0.13	53000	906.29	7.59
6	928370	131.40	7065.22	271.74	0.06	0.10	51700	743.36	6.86
7	1246954	156.70	7957.59	306.06	0.06	0.11	66900	834.34	8.91
8	1566419	126.50	12382.76	476.26	0.10	0.17	43900	827.87	9.17
9	1353088	103.70	13048.10	501.85	0.10	0.18	39600	812.32	8.88
10	1007295	170.46	5909.27	227.28	0.05	0.08	65000	654.88	8.19
Mean							53630	806.84	8.26
SD							8693.3	86.99	0.94

Table 4. 10 SUV for Stress normal myocardial perfusion scan in female patients

Pat no.	Total counts	volume (cc)	counts /cc	CPM/cc	Act: Conc	RC apply Act: Con	Body Wt(g)	Inj dose (MBq)	SUV
1	1249028	135.8	9197.56	353.75	0.07	0.13	48200	748.95	8.27
2	999944	135.4	7385.11	284.04	0.06	0.10	51900	778.83	6.87
3	1574128	142.6	11038.77	424.57	0.09	0.15	56100	836.65	10.34
4	1497061	157.9	9481.07	364.66	0.07	0.13	60000	805.93	9.86
5	1377230	148.2	9293.05	357.42	0.07	0.13	53000	821.31	8.37
6	885578	140.2	6316.53	242.94	0.05	0.09	51700	719.94	6.33
7	1058526	150.9	7014.75	269.80	0.06	0.10	66900	789.39	8.30
8	1606752	118.3	13582.01	522.39	0.11	0.19	43900	801.20	10.39
9	1548582	133.4	11608.56	446.48	0.09	0.16	39600	749.64	8.56
10	795595	175.8	4525.57	174.06	0.04	0.06	65000	654.88	6.27
Mean							53630	770.67	8.36
SD							8693	54.17	1.53

*Table 4. 11 SUV for Rest normal myocardial perfusion scan in male patients*

Pat no.	Total counts	volume (cc)	counts /cc	CPM/cc	Act:Conc (MBq/cc)	RC apply Act: Con	Body Wt(g)	Injdose (MBq)	SUV
1	1313014	200	6565.07	252.50	0.052	0.092	68000	877.11	7.11
2	1066769	153.9	6931.57	266.60	0.055	0.097	69500	830.42	8.10
3	1501670	209	7185.02	276.35	0.057	0.100	56000	759.42	7.40
4	1474517	125.4	11758.5	452.25	0.093	0.164	43000	793.80	8.89
5	1277333	196.3	6507.05	250.27	0.051	0.091	59500	787.86	6.86
6	1444425	245.2	5890.80	226.57	0.046	0.082	49200	682.85	5.93
7	2042754	213.2	9581.40	368.52	0.076	0.134	57100	906.49	8.43
8	1404815	174.9	8032.10	308.93	0.063	0.112	89100	890.05	11.23
9	1624682	193	8418.04	323.77	0.066	0.118	69000	901.83	8.99
10	1314345	212	6570.07	251.50	0.052	0.092	72300	897.54	7.38
Mean							63270	832.74	8.03
SD							12477	71.44	1.40

*Table 4. 12 SUV for Stress normal myocardial perfusion scan in male patients*

Pat no.	Total counts	Volume (cc)	Counts /cc	CPM/cc	Act: Conc (MBq/cc)	RC apply Act: Con	Body Wt(g)	Inj:dose (MBq)	SUV
1	1128844	256.7	4397.52	169.14	0.03	0.06	68000	683.53	6.11
2	1200467	187.4	6405.91	246.38	0.05	0.09	69500	719.83	8.64
3	1340244	215.1	6230.79	239.65	0.05	0.09	56000	749.05	6.50
4	1564707	135.9	11513.66	442.83	0.09	0.16	43000	671.77	10.29
5	1246516	216.7	5752.27	221.24	0.05	0.08	59500	707.60	6.75
6	1809098	237.7	7610.85	292.72	0.06	0.11	49200	827.02	6.32
7	1632315	233.6	6987.65	268.76	0.06	0.10	57100	771.05	7.23
8	854951	171.73	4978.46	191.48	0.04	0.07	89100	619.96	9.99
9	965619	183	5276.61	202.95	0.04	0.07	69000	634.39	8.01
10	1127873	258	4409.55	169.60	0.03	0.06	72300	683.53	6.51
Mean							63270	706.77	7.64
SD							12477	59.69	1.46



In the second method, 20 segments of left ventricular wall were drawn by Image J software based on the resliced image. The segments were divided into three main coronary arteries of the heart according to the myocardial perfusion 20 segments scoring methods as shown in figure 4.9. Left anterior descending artery includes segments 1, 2, 3, 7, 8, 9, 13, 14, 19, 20; left circumflex artery includes segments 5, 6, 11, 12, 17, 18; right coronary artery includes segments 4, 10, 15, 16. The cardiac volume was derived from the pixel area of SPECT reconstructed images with image J software. The exchange unit of 0.085 for one pixel was calculated from 281.23 mm x 281.23mm (length of reconstructed image) divided by 64 x 64 (matrix size) = 4.394 mm (length) and then converted to the volume (mm<sup>3</sup>) in term of cc. The example of 20 segments SUV is shown in table 4.13. The example of three main coronary arteries in which related segments are shown in Table 4.14. Myocardial Perfusion SPECT 20-Segment Scoring Diagrammatic representation of the segmental division of the SPECT slices and assignment of individual segments to individual coronary arteries using the 20-segment model is shown in figure 4.9 (14) .

LAD=left anterior descending coronary artery; LCX=left circumflex coronary artery; RCA=right coronary artery

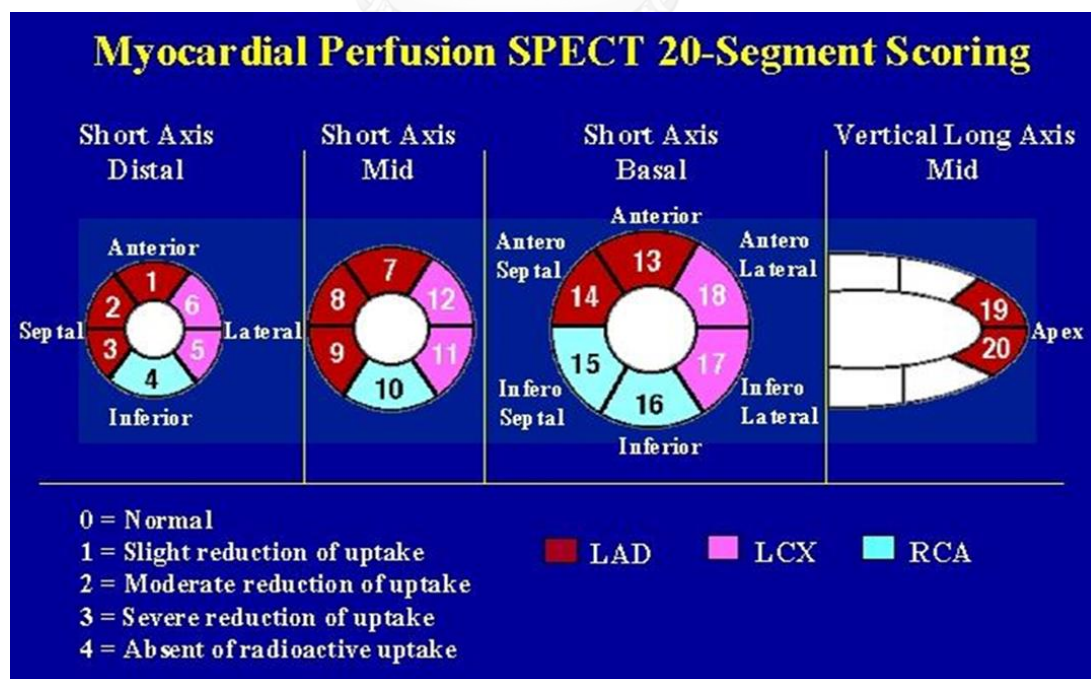


Figure 4.9 Myocardial Perfusion SPECT 20-Segment Scoring template

Table 4. 13 The example of rest SUV for normal myocardial perfusion scan by using Image J

Seg: no.	Area	Total counts	Volume (cc)	Counts /cc	CPM/CC	Act: Con (MBq/cc)	RC apply Act: Con	Inj:act (MBq)	Body Wt (g)	SUV
1	15	9574	1.28	7509.02	288.81	0.06	0.10	69500	830.42	8.78
2	15	9829	1.28	7709.02	296.50	0.06	0.11	69500	830.42	9.01
3	13	8600	1.11	7782.81	299.34	0.06	0.11	69500	830.42	9.10
4	14	7929	1.19	6663.03	256.27	0.05	0.09	69500	830.42	7.79
5	11	6427	0.94	6873.80	264.38	0.05	0.10	69500	830.42	8.03
6	11	6662	0.94	7125.13	274.04	0.06	0.10	69500	830.42	8.33
7	28	14557	2.38	6116.39	235.25	0.05	0.09	69500	830.42	7.15
8	29	17815	2.47	7227.18	277.97	0.06	0.10	69500	830.42	8.45
9	28	16521	2.38	6941.60	266.98	0.05	0.10	69500	830.42	8.11
10	29	16447	2.47	6672.21	256.62	0.05	0.09	69500	830.42	7.80
11	29	16846	2.47	6834.08	262.85	0.05	0.10	69500	830.42	7.99
12	30	16013	2.55	6279.61	241.52	0.05	0.09	69500	830.42	7.34
13	28	15508	2.38	6515.97	250.61	0.05	0.09	69500	830.42	7.62
14	29	15261	2.47	6191.08	238.12	0.05	0.09	69500	830.42	7.24
15	28	13453	2.38	5652.52	217.40	0.04	0.08	69500	830.42	6.61
16	29	17294	2.47	7015.82	269.84	0.06	0.10	69500	830.42	8.20
17	29	15783	2.47	6402.84	246.26	0.05	0.09	69500	830.42	7.48
18	30	16852	2.55	6608.63	254.18	0.05	0.09	69500	830.42	7.72
19	23	12486	1.96	6386.70	245.64	0.05	0.09	69500	830.42	7.46
20	23	11052	1.96	5653.20	217.43	0.04	0.08	69500	830.42	6.61
									Mean	7.84
									Max	9.10
									Min	6.61

Table 4. 14 (a) Example of rest SUV in LAD, LCX and RCA and related segments for normal scan

Seg no.	Rest				Stress						
	SUV	Seg: no.	SUV	Seg no.	SUV	Seg no.	SUV	Seg no.			
	LAD	LCX	RCA	LAD	LCX	RCA	LAD	LCX	RCA		
1	8.78	5	8.03	4	7.79	1	8.76	5	8.17	4	7.89
2	9.01	6	8.33	10	7.80	2	9.12	6	8.13	10	8.67
3	9.10	11	7.99	15	6.61	3	9.42	11	7.99	15	7.05
7	7.15	12	7.34	16	8.20	7	7.11	12	7.45	16	8.51
8	8.45	17	7.48	avg	7.60	8	9.23	17	7.63	avg	8.03
9	8.11	18	7.72			9	9.00	18	7.25		
13	7.62	avg	7.82			13	7.59	avg	7.77		
14	7.24					14	8.44				
19	7.46					19	8.50				
20	6.61					20	8.54				
avg	7.95					avg	8.57				

*Table 4.14 (b). Average SUV for three vessels of the heart in normal myocardial perfusion in 10 patients by using Image J*

Pt. no.	Rest study			Stress study		
	LAD	LCX	RCA	LAD	LCX	RCA
1	7.95	7.82	7.6	8.57	7.77	8.03
2	8.95	9.4	8.11	7.7	8.84	7.9
3	6.19	6.82	5.99	6.39	6.38	6.72
4	6.55	6.84	6.45	6.9	7.09	6.68
5	7.87	8.63	8.38	9.45	10.23	9.91
6	9.9	10.15	10.18	9.4	10.7	9.05
7	7.75	8.77	8.69	7.26	6.74	7.29
8	6.77	7.01	6.29	6.25	6.29	5.47
9	6.89	7.39	7.54	7.57	7.43	7.57
10	8.17	8.68	6.87	7.24	8.96	6.96
Average	7.70	8.15	7.61	7.67	8.04	7.56
SD	1.1	1.2	1.3	1.1	1.6	1.2

#### 4.5 Standardized Uptake Value of abnormal myocardial perfusion scan

In the abnormal myocardial perfusion scan, the data analysis was also carried out with two methods to determine the SUV(17). In the first method, the left ventricle of the myocardium was drawn by a soft auto ROI contour reconstruction algorithm with ISO 50 %. The example of abnormal patients who underwent myocardial perfusion scan and coronary angiography are illustrated in Appendix B. In this study, the location, and extent of significant coronary artery disease were assessed in 27 patients with abnormal MPI who underwent invasive cardiac angiography (CAG). The average and standard deviation of patient weight were  $70204 \pm 15144$  g. The average and standard deviation of injected dose was  $767.39 \pm 87.91$  MBq. The average and standard deviation of SUV in all patients were  $9.47 \pm 2$  ranged from 14.63 to 6.53 for rest scan and  $8.92 \pm 1.99$  ranged from 13.6 to 5.96 for stress scan, respectively. The mean and SD of Standardized Uptake Value of abnormal myocardial perfusion scan for rest and stress studies in male patients were  $9.5 \pm 2$  (13.6-7.1) and  $9.8 \pm 2$  (14.5-6.8) respectively. The mean and SD of Standardized Uptake Value of abnormal

myocardial perfusion scan for rest and stress studies in female patients were  $9.2 \pm 2.1$  (14.6-6.5) and  $8.3 \pm 2$  (12.3-5.9), respectively.

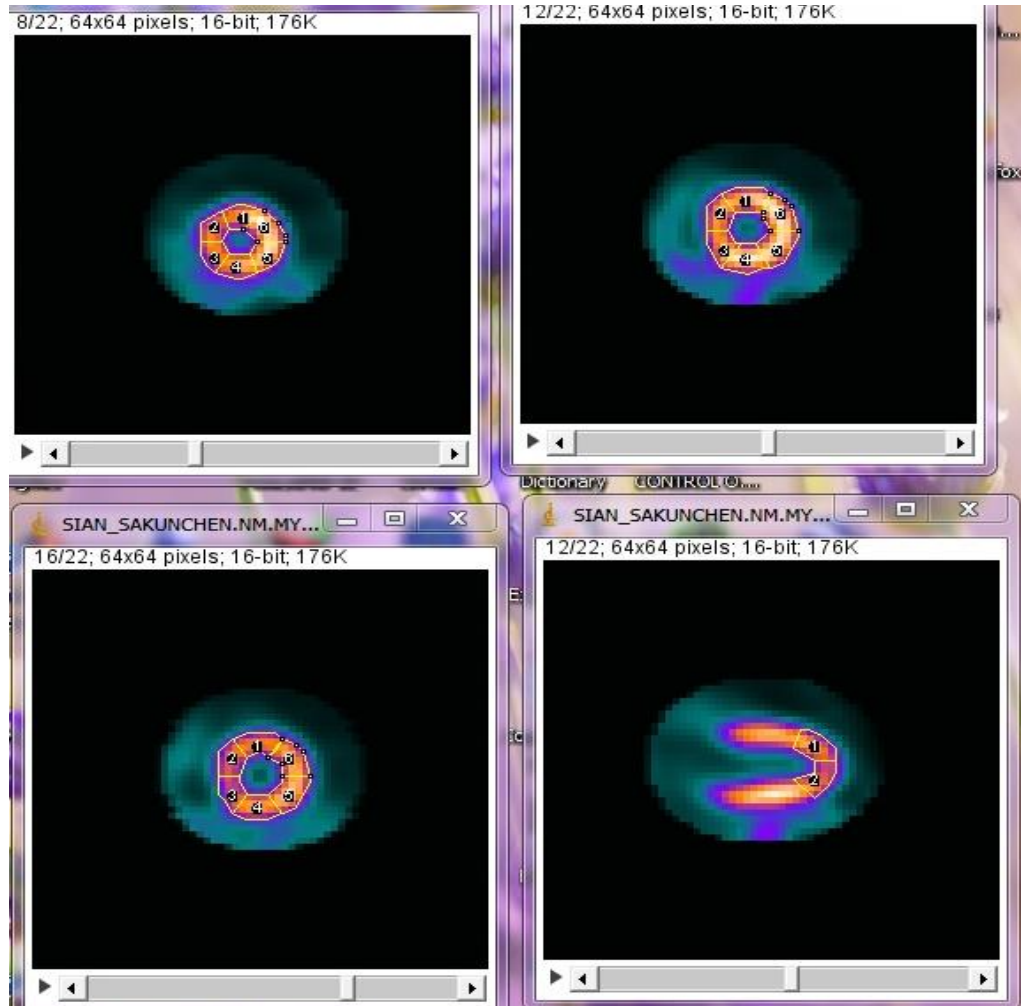


Figure 4. 10 The sample image of 20 segments drawn by Image J software

In the second method, 20 segments of left ventricular wall were drawn by Image J software based on the reconstructed slices. The segments were divided into three main coronary arteries of the heart according to the myocardial perfusion 20 segments scoring methods. Left anterior descending artery includes segments 1, 2, 3, 7, 8, 9, 13, 14, 19, 20; left circumflex artery includes segments 5, 6, 11, 12, 17, 18; right coronary artery includes segments 4, 10, 15, 16. The example of ROI drawn by image was illustrated in figure 4.10. The cardiac volume was derived from the pixel area on the image J software. The exchange unit of 0.085 for one pixel was calculated from  $281.23 \text{ mm}/64 = 0.4394 \text{ cm}$  and then converts to the volume in term of cc

Z scoring method  $(\text{mean SUV}_{\text{pt}} - \text{mean SUV}_{\text{normal}})/\text{SD}$  was used to evaluate differences between normal myocardial perfusion measurement and abnormal myocardial perfusion measurement. The higher negative SUV score means abnormal and the lower negative SUV score means normal. Cut off of the estimated z score z score is (-2) (14). After that, SUV results from each patient were compared to myocardial perfusion scan report and coronary angiography result (CAG). CAG result was used as a gold standard to define diagnostic index. Artery stenosis  $\geq 50\%$  was considered as abnormal. Table 4.15 and 4.16 show average SUV for rest and stress normal myocardial perfusion scan. Table 4.17, 4.18, 4.19, 4.20, 4.21, 4.22, 4.23 and 4.24 show the SUV and Score for rest and stress abnormal myocardial perfusion scan. The score on each segment of left ventricle was compared with MPI result which is extracted from retrospective report (not from images). The stress SUV from patient number 8, 12 and 21 are not shown in the table because of some errors at the time of reconstruction and acquisition.

Table 4. 15 Average SUV for rest normal myocardial perfusion scan (4 male patients and 6 female patients)

Segment	pt1	pt2	pt3	pt4	pt5	pt6	pt7	pt8	pt9	pt10	Average	SD
<b>1</b>	8.78	9.33	7.01	6.52	7.48	10.17	8.77	6.61	7.83	9.37	<b>7.53</b>	1.27
<b>2</b>	9.01	9.43	7.56	7.20	8.39	9.26	9.09	7.00	8.26	8.95	<b>7.83</b>	0.89
<b>3</b>	9.10	9.80	8.25	6.67	8.00	10.33	10.01	7.41	8.12	9.35	<b>8.19</b>	1.20
<b>7</b>	7.15	10.47	6.77	6.92	7.85	10.04	9.36	7.40	8.14	9.52	<b>8.24</b>	1.37
<b>8</b>	8.45	9.51	6.00	7.31	9.04	9.99	10.00	8.37	8.57	9.79	<b>8.64</b>	1.28
<b>9</b>	8.11	9.13	6.63	6.64	8.05	10.52	10.27	7.51	7.68	9.67	<b>8.47</b>	1.41
<b>13</b>	7.62	7.85	5.05	6.35	8.55	10.55	7.96	6.65	7.87	7.86	<b>8.12</b>	1.45
<b>14</b>	7.24	5.65	2.38	5.93	7.38	9.25	6.15	4.03	5.94	3.87	<b>6.53</b>	1.98
<b>19</b>	7.46	9.36	6.37	5.81	6.98	10.00	8.79	6.39	6.97	8.20	<b>8.67</b>	1.40
<b>20</b>	6.61	9.02	5.88	6.19	6.97	8.93	7.75	6.37	6.89	8.17	<b>8.43</b>	1.13
5	8.03	9.46	7.58	6.70	8.44	9.43	9.10	6.81	7.33	9.59	<b>7.95</b>	1.12
6	8.33	10.21	7.27	6.71	7.56	10.46	9.77	7.20	7.76	9.47	<b>8.25</b>	1.38
11	7.99	9.94	6.94	6.76	9.22	10.25	9.52	7.15	8.18	9.75	<b>8.79</b>	1.33
12	7.34	10.40	6.93	7.70	8.77	10.18	9.89	8.04	8.45	10.19	<b>9.08</b>	1.30
17	7.48	8.61	6.05	6.36	8.79	10.53	8.81	6.20	7.54	8.27	<b>8.69</b>	1.42
18	7.72	7.79	6.16	6.79	8.97	10.10	8.78	6.66	7.39	8.69	<b>8.82</b>	1.22
4	7.79	9.45	7.49	6.44	8.13	9.98	8.71	6.85	7.27	9.34	<b>7.77</b>	1.19
10	7.80	9.77	7.69	6.95	9.26	10.83	10.24	7.34	8.21	9.80	<b>8.90</b>	1.35
15	6.61	5.00	3.00	5.32	7.04	9.76	8.51	4.84	5.41	4.01	<b>6.77</b>	2.06
16	8.20	8.20	5.79	7.11	9.11	10.17	8.69	6.16	7.54	6.87	<b>8.53</b>	1.36

Table 4. 16 Average SUV for stress normal myocardial perfusion scan (4 male patients and 6 female patients)

Segment	pt1	pt2	pt3	pt4	pt5	pt6	pt7	pt8	pt9	pt10	Average	SD
<b>1</b>	8.76	7.73	6.72	6.54	8.30	10.68	8.74	6.17	8.16	8.07	<b>7.35</b>	<b>1.32</b>
<b>2</b>	9.12	7.14	6.59	7.41	10.27	10.57	9.59	6.52	8.72	7.73	<b>7.79</b>	<b>1.49</b>
<b>3</b>	9.42	7.75	6.86	7.30	9.68	11.72	9.69	6.65	9.08	8.26	<b>8.13</b>	<b>1.58</b>
<b>7</b>	7.11	8.51	6.04	6.77	9.18	11.63	8.21	6.72	9.14	8.52	<b>8.08</b>	<b>1.63</b>
<b>8</b>	9.23	8.23	6.67	7.60	10.62	10.67	7.85	7.43	9.32	9.05	<b>8.61</b>	<b>1.34</b>
<b>9</b>	9.00	7.63	6.94	6.97	9.10	11.14	8.72	6.59	8.53	8.27	<b>8.35</b>	<b>1.35</b>
<b>13</b>	7.59	8.39	6.25	6.64	10.51	10.38	5.40	5.22	7.29	7.53	<b>8.02</b>	<b>1.83</b>
<b>14</b>	8.44	6.82	5.11	5.97	8.16	6.70	4.08	3.18	4.65	4.80	<b>6.54</b>	<b>1.73</b>
<b>19</b>	8.50	7.34	6.60	7.10	9.39	10.62	7.91	5.85	7.82	8.41	<b>8.96</b>	<b>1.38</b>
<b>20</b>	8.54	7.42	6.13	6.69	9.28	9.44	7.27	6.25	7.57	7.24	<b>8.71</b>	<b>1.16</b>
5	8.17	7.88	6.51	7.41	9.85	9.40	8.60	6.35	8.47	7.90	<b>7.77</b>	<b>1.12</b>
6	8.13	8.53	6.84	7.37	8.90	10.60	9.41	6.52	8.32	8.17	<b>8.07</b>	<b>1.21</b>
11	7.99	9.10	5.98	6.95	10.89	10.64	9.23	6.74	9.47	8.73	<b>8.79</b>	<b>1.64</b>
12	7.45	9.23	5.85	7.49	10.43	11.14	8.72	7.44	8.76	8.96	<b>8.86</b>	<b>1.56</b>
17	7.63	9.33	6.34	6.63	10.49	10.05	7.58	6.25	7.66	8.73	<b>8.88</b>	<b>1.52</b>
18	7.25	8.99	6.77	6.68	10.81	10.73	6.75	6.30	7.43	8.96	<b>8.97</b>	<b>1.69</b>
4	7.89	8.06	6.05	7.01	10.09	11.13	8.89	6.23	8.29	7.73	<b>7.76</b>	<b>1.59</b>
10	8.67	8.46	7.78	7.16	10.54	11.10	9.33	6.81	10.12	8.27	<b>8.93</b>	<b>1.43</b>
15	7.05	6.51	5.69	5.54	8.23	6.96	5.49	3.63	5.03	4.35	<b>6.68</b>	<b>1.37</b>
16	8.51	8.58	7.39	6.99	10.76	9.06	7.29	5.47	7.57	6.97	<b>8.60</b>	<b>1.44</b>



*Table 4. 17 The result of Rest SUV in 27 abnormal myocardial perfusion scan for 20 segments*

Pat: no.	Left Anterior Descending (segments) SUV									Left Circumflex (segments) SUV									Right Coronary (seg:) SUV					
	1	2	3	7	8	9	13	14	19	20	5	6	11	12	17	18	4	10	15	16				
1	6.9	7.0	7.7	8.2	8.3	8.3	7.2	6.1	7.2	7.5	7.9	7.5	10.3	9.4	9.0	8.1	8.3	10.6	6.1	8.2				
2	7.3	7.5	9.1	7.9	9.4	9.8	5.7	4.3	7.1	7.9	9.1	8.0	9.6	7.5	8.0	6.0	10.2	10.5	6.6	8.6				
3	6.6	5.9	6.9	7.7	7.6	7.4	8.1	5.7	5.8	6.1	8.2	8.2	8.1	9.4	7.7	8.3	7.2	6.6	3.9	5.0				
4	4.2	4.1	5.1	8.2	8.3	9.0	7.5	5.5	4.4	2.2	8.5	7.9	7.7	8.9	7.1	7.0	7.2	8.5	5.1	7.4				
5	3.2	2.5	3.7	5.4	4.9	6.3	4.5	2.7	3.6	2.0	5.6	5.2	5.9	5.5	5.6	5.5	5.5	6.8	3.4	5.9				
6	6.7	1.7	3.7	6.4	6.2	7.5	7.2	7.0	4.9	2.6	6.9	7.9	6.4	6.1	6.6	5.8	5.9	6.7	6.2	5.8				
7	9.3	11.0	10.8	10.7	10.9	10.4	8.9	5.3	9.4	9.8	10.2	9.5	10.7	10.8	8.4	9.8	9.5	10.8	6.9	8.9				
8	7.5	8.6	9.3	8.3	10.6	11.0	7.5	5.5	9.1	9.6	9.9	9.1	10.5	10.3	9.1	8.9	8.9	10.8	7.9	9.9				
9	5.3	6.4	7.4	6.8	6.3	6.5	4.0	2.1	5.5	4.6	8.8	7.0	8.7	7.8	6.9	6.3	9.1	8.3	3.0	4.1				
10	9.7	11.3	13.1	9.9	12.1	12.8	6.8	4.9	11.2	11.7	10.2	10.6	12.3	12.0	8.8	8.8	11.0	13.2	7.8	8.4				
11	6.2	7.3	8.4	7.5	8.4	8.2	6.7	5.1	7.5	7.1	6.9	6.8	8.0	8.1	6.7	7.0	7.4	8.4	5.2	6.9				
12	10.9	11.1	12.2	11.9	12.6	12.0	11.6	10.1	10.8	9.3	10.0	10.9	9.8	11.3	9.3	10.4	10.7	11.3	9.6	9.8				
13	12.7	12.2	12.4	12.2	12.6	11.3	10.8	5.7	12.7	12.3	13.4	13.2	12.6	12.6	10.1	11.1	13.5	12.0	4.8	8.7				
14	7.6	8.7	9.9	8.3	10.6	11.9	9.7	10.7	9.6	9.4	8.7	8.5	9.7	8.6	10.0	9.9	9.3	10.2	11.0	10.1				

Table 4. 18 The result of Rest SUV in 27 abnormal myocardial perfusion scan for 20 segments (cont.)

Pat: no.	Left Anterior Descending (segments) SUV							Left Circumflex (segments) SUV					Right Coronary (seg:) SUV								
	1	2	3	7	8	9	13	14	19	20	5	6	11	12	17	18	4	10	15	16	
15	7.3	8.5	10.1	10.1	10.1	9.5	8.9	8.3	7.5	8.0	8.1	8.5	7.7	9.2	8.9	7.5	6.7	9.6	9.0	5.0	8.9
16	5.5	6.6	6.9	6.5	7.1	7.1	5.0	2.6	5.7	5.2	5.2	6.6	6.3	6.4	7.4	6.5	5.9	6.3	6.7	3.3	5.5
17	10.1	10.9	10.6	10.5	10.3	9.6	7.2	4.1	9.9	8.5	8.5	9.0	9.7	9.7	11.1	8.6	8.4	8.9	10.0	5.5	8.9
18	7.6	6.9	8.5	6.0	6.7	6.6	5.3	6.5	5.8	6.6	6.6	5.9	8.2	5.9	7.2	5.9	6.4	6.6	6.6	6.7	6.9
19	6.3	6.7	8.8	8.4	8.3	7.2	8.9	4.4	7.4	6.7	6.7	8.5	7.1	8.3	9.1	8.9	10.6	7.5	9.4	4.5	8.2
20	9.3	8.9	9.9	9.8	10.2	9.9	6.3	4.7	7.9	7.7	7.7	9.0	9.4	9.7	9.1	8.3	7.9	9.1	10.4	6.3	8.1
21	8.3	9.8	10.1	9.0	11.0	10.7	8.9	7.3	8.8	9.0	9.0	7.8	7.6	9.2	7.1	8.9	8.8	9.6	10.9	8.4	10.2
22	12.9	16.4	17.2	15.1	17.9	16.4	13.4	11.6	15.6	13.0	13.0	11.6	14.0	15.0	16.3	13.3	13.6	12.7	15.1	9.6	11.6
23	10.1	10.8	11.0	8.8	8.0	10.3	5.6	2.7	10.8	10.3	10.3	11.7	10.7	10.9	10.0	9.5	8.6	10.4	9.5	5.5	8.1
24	8.4	8.5	8.6	8.6	9.1	8.6	8.0	8.1	8.0	7.8	7.8	7.5	7.7	8.0	8.1	7.9	7.5	7.8	8.7	8.5	8.6
25	8.8	7.2	8.6	0.0	8.2	8.5	6.9	5.9	7.6	7.6	7.6	8.2	9.1	8.7	8.6	8.8	7.4	9.2	9.6	6.1	9.2
26	8.1	7.5	8.7	9.4	9.4	9.0	7.6	5.7	7.8	5.5	5.5	9.5	9.1	9.5	10.3	8.6	8.2	8.1	10.0	6.7	9.1
27	5.6	4.8	5.7	5.9	3.8	6.2	4.4	1.6	4.3	3.7	3.7	7.7	7.1	6.6	7.6	4.6	6.2	6.4	6.9	3.9	5.8

Table 4. 19 The result of Rest score in 27 abnormal myocardial perfusion scan for 20 segments

REST Pat. no.	Left Anterior Descending (segments) z- score												Left Circumflex (segments) z- score						Right Coronary (seg.)						CAG % Stenosis	CAG % Steosis
	1	2	3	7	8	9	13	14	19	20	5	6	11	12	17	18	4	10	15	16						
1	0.47	0.97	0.43	0.00	0.24	0.12	0.61	0.20	1.02	0.84	0.08	0.51	1.13	0.26	0.20	0.63	0.45	1.27	0.31	0.26	80	80				
2	0.21	0.32	0.76	0.24	0.61	0.91	1.67	1.11	1.11	0.48	0.99	0.20	0.57	1.22	0.47	2.29	2.01	1.18	0.09	0.03	80	80				
3	0.77	2.21	1.11	0.37	0.79	0.75	0.02	0.40	2.02	2.04	0.22	0.07	0.53	0.23	0.67	0.39	0.46	1.67	1.39	2.60	100	100				
4	2.65	4.17	2.55	0.06	0.28	0.35	0.46	0.52	3.07	5.53	0.53	0.27	0.81	0.15	1.12	1.49	0.51	0.27	0.81	0.86	N	N				
5	3.44	6.00	3.78	2.07	2.90	1.51	2.49	1.92	3.62	5.72	2.13	2.20	2.19	2.72	2.16	2.70	1.92	1.58	1.63	1.96	40	80				
6	0.64	6.94	3.70	1.34	1.88	0.70	0.66	0.22	2.69	5.21	0.96	0.26	1.82	2.29	1.51	2.48	1.56	1.65	0.25	2.05	N	N				
7	1.39	3.57	2.16	1.81	1.76	1.38	0.54	0.60	0.54	1.26	2.03	0.88	1.42	1.31	0.18	0.84	1.44	1.42	0.07	0.24	N	N				
8	0.05	0.85	0.96	0.05	1.53	1.80	0.40	0.54	0.30	1.04	1.77	0.58	1.28	0.94	0.32	0.08	0.99	1.42	0.56	1.02	N	N				
9	1.77	1.59	0.63	1.05	1.83	1.38	2.87	2.26	2.27	3.43	0.78	0.91	0.10	1.01	1.27	2.09	1.13	0.41	1.83	3.29	40	40				
10	1.70	3.90	4.11	1.23	2.70	3.09	0.92	0.80	1.81	2.92	2.02	1.67	2.65	2.27	0.08	0.00	2.68	3.19	0.52	0.08	70	70				
11	1.04	0.55	0.14	0.56	0.16	0.17	1.01	0.70	0.87	1.20	0.98	1.02	0.57	0.76	1.39	1.52	0.30	0.38	0.75	1.23	N	N				
12	2.66	3.67	3.33	2.67	3.08	2.52	2.40	1.81	1.53	0.73	1.81	1.93	0.75	1.72	0.44	1.33	2.51	1.81	1.39	0.96	90	90				
13	4.08	4.90	3.47	2.90	3.09	1.99	1.84	0.42	2.90	3.44	4.91	3.56	2.83	2.72	0.97	1.90	4.78	2.27	0.96	0.10	N	N				
14	0.03	0.95	1.45	0.02	1.51	2.40	1.12	2.13	0.67	0.89	0.66	0.21	0.66	0.39	0.89	0.92	1.29	0.93	2.06	1.19	50	50				

Table 4. 20 The result of Rest score in 27 abnormal myocardial perfusion scan for 20 segments (Cont.)

REST Pat: no.	Left Anterior Descending (segments) z-score												CAG					Left Circumflex (segments z- score					CAG					Right Coronary (seg:) CAG						
	1	2	3	7	8	9	13	14	19	20	% Stenosis	5	6	11	12	17	18	% Stenosis	4	10	15	16	% Stenosis	5	6	11	12	17	18	% Stenosis	4	10	15	16
15	0.22	0.71	1.59	1.34	0.68	0.32	0.10	0.51	0.48	0.31	70	0.52	0.37	0.31	0.14	0.82	1.72	100	1.55	0.08	0.88	0.25	70	1.55	0.37	0.31	0.14	0.82	1.72	100	1.55	0.08	0.88	0.25
16	1.62	1.37	1.08	1.23	1.24	0.95	2.13	1.97	2.14	2.91	50	1.18	1.43	1.80	1.26	1.55	2.36	10	1.26	1.64	1.68	2.26	30	1.26	1.43	1.80	1.26	1.55	2.36	10	1.26	1.64	1.68	2.26
17	2.02	3.46	2.02	1.64	1.28	0.82	0.65	1.21	0.88	0.04	N	0.91	1.06	0.66	1.54	0.06	0.35	N	0.94	0.81	0.61	0.30	N	0.94	1.06	0.66	1.54	0.06	0.35	N	0.94	0.81	0.61	0.30
18	0.02	1.06	0.27	1.62	1.55	1.30	1.97	0.01	2.05	1.66	90	1.87	0.00	2.19	1.48	1.97	1.96	99	0.97	1.70	0.04	1.21	100	0.97	1.87	0.00	2.19	1.48	1.96	99	0.97	1.70	0.04	1.21
19	0.97	1.23	0.53	0.12	0.26	0.93	0.51	1.09	0.87	1.52	N	0.49	0.83	0.35	0.00	0.18	1.43	N	0.21	0.34	1.09	0.28	N	0.21	0.49	0.83	0.35	0.00	1.43	N	0.21	0.34	1.09	0.28
20	1.37	1.26	1.43	1.11	1.21	0.99	1.25	0.92	0.58	0.66	80	0.91	0.83	0.67	0.01	0.25	0.78	N	1.16	1.10	0.23	0.33	80	0.91	0.83	0.67	0.01	0.25	0.78	N	1.16	1.10	0.23	0.33
21	0.59	2.23	1.63	0.52	1.85	1.56	0.55	0.41	0.13	0.51	90	0.17	0.49	0.34	1.53	0.13	0.04	20	1.54	1.50	0.78	1.21	60	0.17	0.49	0.34	1.53	0.13	0.04	20	1.54	1.50	0.78	1.21
22	4.19	9.67	7.52	4.99	7.24	5.60	3.66	2.59	4.97	4.05	N	3.26	4.18	4.66	5.58	3.25	3.91	N	4.12	4.55	1.36	2.27	100	3.26	4.18	4.66	5.58	3.25	3.91	N	4.12	4.55	1.36	2.27
23	2.02	3.39	2.34	0.40	0.47	1.29	1.74	1.95	1.50	1.67	70	3.32	1.80	1.55	0.74	0.55	0.18	N	2.19	0.47	0.63	0.33	80	3.32	1.80	1.55	0.74	0.55	0.18	N	2.19	0.47	0.63	0.33
24	0.65	0.71	0.38	0.26	0.37	0.11	0.11	0.77	0.50	0.56	90	0.45	0.38	0.56	0.75	0.55	1.09	90	0.05	0.12	0.84	0.05	N	0.45	0.38	0.56	0.75	0.55	1.09	90	0.05	0.12	0.84	0.05
25	0.97	0.66	0.31	0.17	0.37	0.01	0.81	0.33	0.76	0.76	100	0.21	0.61	0.07	0.36	0.08	1.18	80	1.23	0.52	0.34	0.50	50	0.21	0.61	0.07	0.36	0.08	1.18	80	1.23	0.52	0.34	0.50
26	0.42	0.40	0.44	0.86	0.57	0.40	0.34	0.42	0.65	2.63	100	1.36	0.61	0.51	0.92	0.06	0.48	N	0.31	0.80	0.04	0.40	N	1.36	0.61	0.51	0.92	0.06	0.48	N	0.31	0.80	0.04	0.40
27	1.51	3.40	2.07	1.71	3.79	1.61	2.58	2.51	3.13	4.18	100	0.25	0.84	1.62	1.17	2.89	2.18	N	1.16	1.48	1.39	2.04	30	0.25	0.84	1.62	1.17	2.89	2.18	N	1.16	1.48	1.39	2.04

Gold standard CAG ( $\geq 50\%$  stenosis) defines abnormal

Table 4. 21 The result of stress SUV in 27 abnormal myocardial perfusion scan for 20 segments

Pat: no.	Left Anterior Descending (segments) SUV																Left Circumflex (segments) SUV				Right Coronary (segments) SUV			
	1	2	3	7	8	9	13	14	19	20	5	6	11	12	17	18	4	10	15	16				
1	4.4	3.8	5.9	8.1	6.3	7.1	8.4	7.7	6.4	6.5	10.2	8.7	11.0	10.7	10.2	9.3	8.6	10.9	7.3	10.4				
2	5.5	7.0	7.7	5.5	7.4	8.1	4.9	4.5	5.1	5.4	5.7	5.0	6.2	4.5	6.0	4.1	6.5	8.3	5.2	6.5				
3	3.3	2.9	4.3	6.5	5.6	5.7	6.6	5.2	2.9	4.6	5.9	4.5	7.2	8.7	6.6	6.8	4.5	6.0	3.2	3.5				
4	5.1	4.5	5.7	9.3	9.8	9.9	7.7	5.0	5.2	2.6	9.3	8.5	8.5	9.1	7.6	7.5	8.9	9.2	4.5	7.5				
5	3.6	2.2	3.1	5.0	3.9	6.1	5.4	3.7	4.4	2.2	5.1	5.2	5.6	5.8	5.2	6.0	5.6	6.6	4.0	5.6				
6	5.5	5.1	5.8	5.5	5.1	5.8	6.0	6.2	0.8	4.5	5.4	5.1	5.4	5.1	5.4	4.9	5.0	5.0	5.4	4.4				
7	10.8	12.5	12.8	10.9	12.5	12.6	11.0	10.7	10.3	10.3	10.9	10.6	11.3	10.6	10.6	9.8	11.0	10.7	10.9	11.3				
9	3.0	2.9	4.5	4.2	4.9	6.5	5.3	3.5	4.4	2.8	5.2	4.1	7.7	6.7	7.0	6.3	6.0	8.5	3.4	6.3				
10	8.8	12.3	14.6	9.2	12.8	14.5	6.9	5.2	10.0	11.6	11.5	10.9	12.5	11.6	9.6	9.7	12.0	13.5	9.2	9.8				
11	5.7	6.1	7.3	7.4	8.1	8.8	7.4	6.3	7.0	7.3	7.1	6.9	8.0	8.9	6.2	7.2	6.7	8.5	5.2	6.3				
13	8.8	11.0	13.0	11.7	13.4	13.7	12.6	12.2	11.3	12.3	10.7	9.6	13.0	12.9	12.3	12.4	13.1	13.8	10.3	12.4				
14	6.9	6.8	7.2	7.1	7.9	8.4	7.2	5.6	7.2	6.2	5.4	6.1	7.3	6.9	7.2	7.2	6.6	8.0	6.9	7.7				

Table 4. 22 The result of stress SUV in 27 abnormal myocardial perfusion scan for 20 segments (cont.)

Pat: no.	Left Anterior Descending (segments) SUV							Left Circumflex (segments) SUV							Right Coronary (segments) SUV					
	1	2	3	7	8	9	13	14	19	20	5	6	11	12	17	18	4	10	15	16
15	6.3	6.0	7.2	6.3	7.9	7.2	6.5	3.9	7.4	6.1	7.0	7.0	6.7	6.8	5.3	5.2	7.1	7.2	4.4	7.0
16	5.6	5.8	7.0	6.5	7.3	7.6	5.9	3.9	6.7	6.0	6.9	6.7	6.3	7.1	6.4	6.3	6.1	6.8	4.3	6.6
17	7.7	8.1	8.0	9.9	9.2	9.2	6.0	3.6	8.4	6.7	7.4	7.9	8.2	9.9	8.8	8.0	6.3	8.9	6.0	7.8
18	7.3	6.5	7.1	6.2	6.5	6.8	6.8	5.7	5.5	5.4	4.2	7.0	5.1	7.1	4.8	6.9	4.0	5.2	5.2	5.9
19	9.9	10.0	11.4	9.3	11.2	10.9	9.4	7.3	8.9	8.8	7.8	9.1	10.0	10.3	10.0	10.5	9.8	11.4	7.1	9.9
20	12.1	11.9	12.9	12.8	14.1	13.1	9.6	9.0	11.1	10.7	13.4	13.0	12.2	13.0	12.1	10.5	12.9	13.6	10.1	11.5
22	11.5	11.6	11.5	12.6	12.2	11.6	10.3	7.9	11.6	9.4	7.6	11.2	9.2	11.9	8.2	10.3	8.8	9.2	7.2	7.7
23	6.3	7.7	7.2	5.9	5.4	6.4	4.2	1.9	6.0	5.5	6.5	6.4	5.9	5.7	5.5	5.2	5.5	5.4	3.3	4.6
24	6.9	7.3	7.9	7.5	8.3	8.5	7.6	7.3	8.0	7.6	6.6	7.0	7.3	7.4	7.4	7.0	6.8	8.0	7.8	8.3
25	5.7	5.4	6.7	7.4	7.9	7.4	5.6	3.6	6.7	6.7	7.0	7.3	8.7	8.0	7.3	6.4	7.5	9.2	4.4	7.1
26	9.0	7.9	8.9	10.0	10.4	10.3	9.7	6.5	8.5	7.8	11.3	10.9	12.2	11.3	10.6	10.5	9.3	12.5	8.9	10.9
27	4.6	4.3	6.3	8.4	6.0	8.3	7.5	4.2	6.8	4.9	9.1	8.6	9.3	9.1	8.3	8.3	8.4	8.5	7.0	7.7

Table 4. 23 The result of stress score in 27 abnormal myocardial perfusion scan for 20 segments

Pat: no.	Left Anterior Descending (segments) z-Score												Left Circumflex (segments) z-Score						Right coronary z-score				CAG % Stenosis
	1	2	3	7	8	9	13	14	19	20	5	6	11	12	17	18	4	10	15	16			
	-2.3	-2.7	-1.4	0.0	-1.7	-0.9	0.2	0.7	-1.9	-1.9	-1.9	-1.9	0.2	0.7	0.2	0.6	1.4	0.4	1.0	80			
2	-1.4	-0.6	-0.3	-1.6	-0.9	-0.2	-1.7	-1.2	-2.8	-2.9	-2.8	-1.9	-2.9	-2.9	-2.9	-0.8	-0.5	-1.1	-1.5	80			
3	-3.05	-3.26	-2.44	-0.95	-2.21	-1.97	-0.76	-0.78	-4.40	-3.52	-4.40	-4.40	-3.52	-3.52	-3.52	-2.02	-2.04	-2.51	3.54	100			
4	-1.70	-2.21	-1.52	0.78	0.87	1.18	-0.15	-0.88	-2.76	-5.27	-2.76	-2.76	-5.27	-5.27	-5.27	0.70	0.20	-1.60	0.79	N			
5	-2.87	-3.73	-3.18	-1.87	-3.54	-1.70	-1.42	-1.62	-3.31	-5.62	-3.31	-3.31	-5.62	-5.62	-5.62	-1.35	-1.64	-1.99	2.06	80			
6	-1.43	-1.78	-1.46	-1.60	-2.59	-1.87	-1.11	-0.21	-5.94	-3.61	-5.94	-5.94	-3.61	-3.61	-3.61	-1.70	-2.72	-0.95	2.92	N			
7	2.58	3.13	2.94	1.76	2.89	3.12	1.61	2.40	1.00	1.34	1.00	1.00	1.34	1.34	1.34	2.05	1.25	3.10	1.86	N			
9	-3.34	-3.25	-2.32	-2.37	-2.73	-1.38	-1.47	-1.73	-3.34	-5.09	-3.34	-3.34	-5.09	-5.09	-5.09	-1.10	-0.31	-2.39	1.59	40			
10	1.06	3.00	4.12	0.70	3.16	4.56	-0.62	-0.79	0.75	2.45	0.75	0.75	2.45	2.45	2.45	2.68	3.22	1.87	0.86	70			
11	-1.25	-1.14	-0.55	-0.41	-0.34	0.30	-0.34	-0.17	-1.44	-1.05	-1.44	-1.44	-1.05	-1.05	-1.05	-0.69	-0.30	-1.06	1.61	N			
13	1.11	2.18	3.11	2.22	3.58	3.97	2.49	3.27	1.67	3.08	1.67	1.67	3.08	3.08	3.08	3.37	3.43	2.62	2.67	N			
14	-0.31	-0.66	-0.61	-0.58	-0.52	0.03	-0.46	-0.52	-1.26	-2.15	-1.26	-1.26	-2.15	-2.15	-2.15	-0.75	-0.65	0.15	0.63	50			

Gold standard CAG (> 50% stenosis) defines abnormal

Table 4. 24 The result of stress score in 27 abnormal myocardial perfusion scan for 20 (c0nt)segments (cont.)

Pat no.	Left Anterior Descending (segments) z-Score										Left Circumflex (segments) z-Score					Right coronary score					CAG % Sten-osis
	1	2	3	7	8	9	13	14	19	20	5	6	11	12	17	18	4	10	15	16	
15	0.77	1.18	0.57	1.08	0.55	-0.85	0.84	1.55	1.16	2.21	0.65	-0.92	1.25	1.32	2.34	2.24	0.41	1.21	1.66	-1.13	70
16	1.35	1.36	0.71	0.98	0.98	-0.54	1.16	1.50	1.65	2.31	0.76	-1.16	1.51	1.13	1.63	1.56	1.05	1.46	1.72	-1.38	30
17	0.29	0.23	0.09	1.14	0.43	0.61	1.10	1.68	0.44	1.76	0.35	-0.14	0.35	0.68	0.08	0.56	0.94	0.05	0.52	-0.57	N
18	0.04	0.86	0.67	1.17	1.58	-1.15	0.66	0.49	2.48	2.81	3.17	-0.86	2.24	1.13	2.69	1.21	2.34	2.64	1.11	-1.88	100
19	1.89	1.45	2.05	0.74	1.96	1.88	0.78	0.47	0.01	0.09	0.01	0.89	0.75	0.93	0.75	0.91	1.30	1.75	0.33	0.90	N
20	3.60	2.75	3.03	2.91	4.07	3.54	0.87	1.41	1.57	1.69	5.05	4.06	2.11	2.68	2.10	0.90	3.23	3.26	2.47	2.02	80
22	3.17	2.57	2.12	2.76	2.70	2.42	1.23	0.76	1.93	0.60	0.20	2.59	0.24	1.95	0.46	0.78	0.62	0.19	0.40	-0.65	100
23	0.83	0.05	0.61	1.32	2.35	-1.44	2.06	2.66	2.13	2.76	1.18	-1.40	1.79	2.05	2.22	2.23	1.43	2.44	2.46	-2.76	80
24	0.36	0.33	0.15	0.36	0.24	0.13	0.25	0.43	0.68	0.94	1.04	-0.86	0.88	0.91	0.99	1.18	0.62	0.69	0.80	-0.18	N
25	1.23	1.61	0.91	0.39	0.54	-0.74	1.34	1.71	1.63	1.77	0.65	-0.64	0.08	0.58	1.05	1.53	0.13	0.19	1.67	-1.06	50
26	1.27	0.08	0.50	1.19	1.31	1.42	0.93	0.03	0.30	0.78	3.15	2.37	2.05	1.58	1.13	0.90	0.99	2.47	1.65	1.60	N
27	-2.1	-2.3	-1.2	0.2	-1.9	-0.1	-0.3	-1.3	-1.6	-3.2	1.2	0.4	0.3	0.2	-0.4	-0.4	0.4	-0.3	0.2	-0.6	30

Gold standard CAG ( $\geq 50\%$  stenosis) defines abnormal



#### 4.6 Relation between SUV and MPI

The results for SUV and MPI with corresponding CAG result are shown in Table 4.25 and 4.26. Using CAG as a gold standard for LAD, LCX and RCA, the vessel stenosis of greater than or equal fifty percent define abnormal. Myocardial Perfusion Imaging use visual interpretation. Percent, specificity, sensitivity and accuracy of SUV and MPI for left anterior descending, left circumflex and right coronary artery in 27 patients are shown in table 4.27, 4.28 and figure 4.11, 4.12, 4.13 and 4.14.

*Table 4. 25 The diagnostic indexes of MPI using visual interpretation in three arteries compare with CAG results*

Vessel	True Positive	True Negative	False Positive	False Negative
LAD	11	1	8	4
LCX	3	9	9	3
RCA	3	10	2	9

*Table 4. 26 The diagnostic indexes of SUV for stress study in LAD, LCX and RCA compared with CAG*

Vessel	LAD	LCX	RCA
Type of Study	Stress	Stress	Stress
True positive	12	3	4
True negative	7	12	10
False positive	2	6	2
False negative	3	3	8

*Table 4. 27 Percent specificity, sensitivity and accuracy of SUV and MPI for three vessels (LAD, LCX and RCA) of the heart in 27 patients*

Type of Test	SUV (Stress)	MPI
Specificity	74 %	51 %
Sensitivity	58 %	52 %
Accuracy	67 %	51 %

*Table 4. 28 Percent specificity, sensitivity and accuracy for LAD, LCX and RCA of the heart in SUV (stress) and MPI*

Type of study	Vessel	Specificity (%)	Sensitivity (%)	Accuracy (%)
SUV (Stress)	LAD	78%	80%	79%
	LCX	67%	50%	65%
	RCA	83%	33%	58%
MPI	LAD	11%	73%	50%
	LCX	50%	50%	50%
	RCA	83%	25%	54%

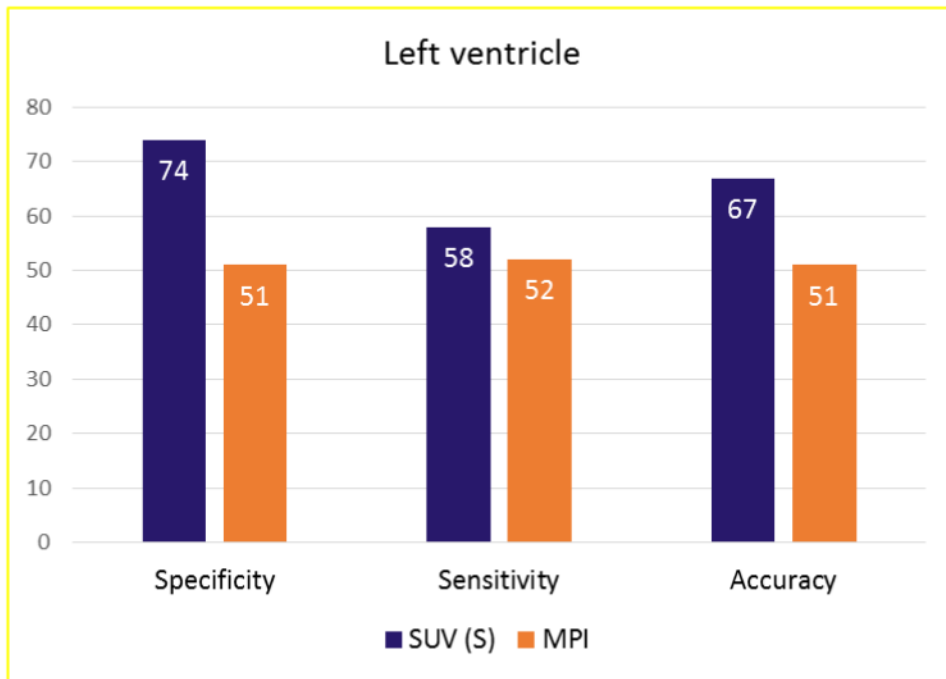


Figure 4. 11 Percent specificity, sensitivity and accuracy for three main vessels (LAD, LCX and RCA) of the heart in SUV (stress) and MPI

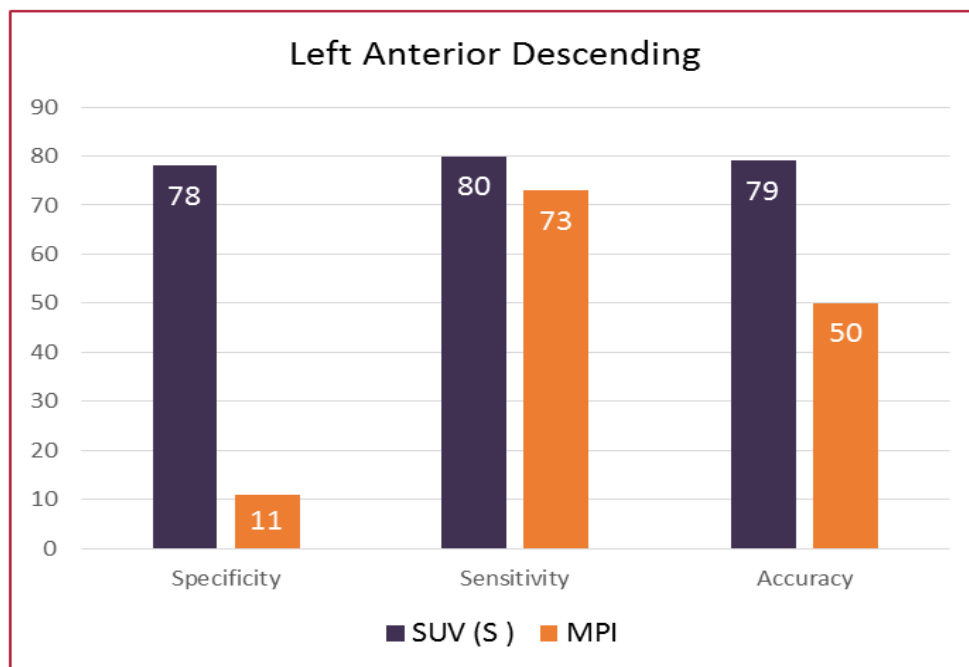


Figure 4. 12 Percent specificity, sensitivity and accuracy for LAD in 27 patients

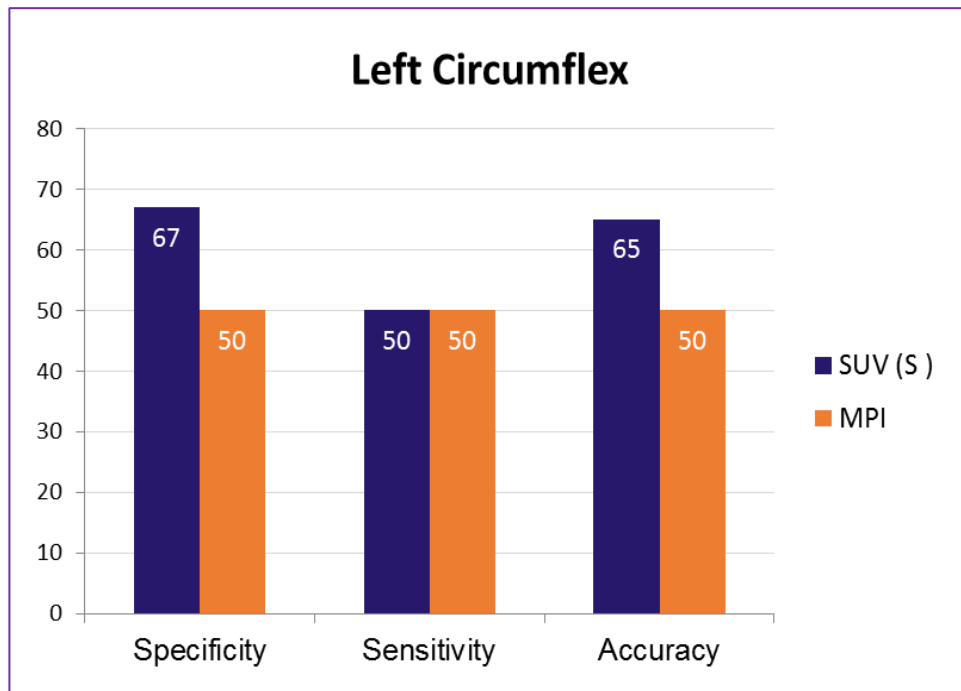


Figure 4. 13 Percent specificity, sensitivity and accuracy for left circumflex in 27 patients

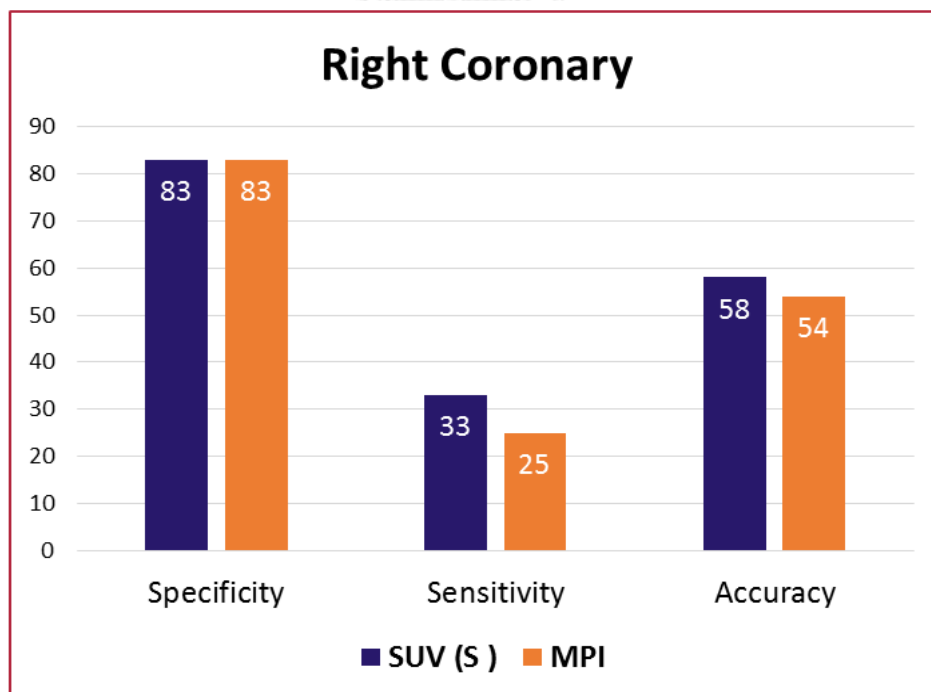


Figure 4. 14 Percent specificity, sensitivity and accuracy for right coronary in 27 patients.

## CHAPTER V

### DISCUSSION AND CONCLUSION

#### 5.1 Discussion

Myocardial perfusion SPECT/CT Tc-99m imaging has been widely used for the diagnosis and prognosis of coronary artery disease. The purpose of this study is to obtain an absolute measurement of tracer activity per specific region of interest such as left ventricular myocardium and its Standardized Uptake Value in order to diminish the pitfalls of myocardial perfusion imaging in detecting balanced ischemia.

An anthropomorphic heart and thorax phantom with 5cc defect was studied. The relative true activity concentration and measured activity concentration were different depending on the percentage of the radioactivity uptake. Concerning the defect activity concentration, overestimation of counts can be seen in 0% and 25% of relative true activity and underestimation can be seen in 50% and 75% of relative true activity (figure 4.5). From this result, the activity concentration in the myocardial perfusion defect cannot be detected linearly. SUV was overestimated if the defect relative uptake was lower or less than fifty percent. SUV was approaching true percentage if the defect relative uptake was more than fifty percent. The reason is possibly due to scatter radiation from the adjacent normal uptake area to the defect area which might affect more on the lower counts area than the higher counts area. Percent difference calculation using maximum count was more linear than using total counts method. The relative percent defect uptake before RC application and after RC application were not changed by using the same RC for defect and normal myocardium because they cancelled each other in the calculation.

However, the relative percent defect uptake before RC application and after RC application were changed by using different RC and different VOI in defect and in normal myocardium (figure 4.6). In this study, scatter correction was not applied. Furthermore, the activity in liver phantom had not been added as in the patients. Thus, for the further study, scatter correction and other factors also should be considered other than recovery coefficient. The measured activity concentration in percent defect uptake was close to the true activity concentration if the different RC

are used in defect and normal myocardium. Among these, percent defect using maximum counts after RC application was more accurate and linear than using total count measurement. However, in the patient study, the region of interest for defect size cannot be determined exactly to calculate the different recovery coefficient. By observing the normal heart and thorax phantom with various volume of interest, the recovery coefficients were not too much different among these (table 4.5). So only one value of recovery coefficient calculated from heart and thorax phantom, can be used in patient study for all regions.

An IEC phantom with six hollow sphere inserts was studied. The recovery coefficient values varied according to the sphere size. The high accurate detected value was obtained in large sphere size and reduced in small sphere. Specific recovery coefficient could not be applied directly to specific defect size because cardiac defect area can not be determined exactly. This is not possible for VOIs of non-spherical shape especially cardiac defect, which behave differently. Thus, the recovery coefficient from the anthropomorphic heart and thorax phantom without defect that assumed to be patient's heart is used instead. The estimated RC values of the sphere phantom and heart phantom are related.

Among 27 patients with abnormal myocardial perfusion scan, six patients showed normal CAG results. Concerning the results between normal and abnormal SUV in our study, five cases (7,11,13,17,19) showed good agreement with CAG result in both rest and stress studies; one case (6) showed good agreement with MPI result including rest and stress study. The diagnostic index for stress SUV and MPI results are shown in tables and graphs in the previous chapter. Percent sensitivity and accuracy of RCA is lower than LAD and LCX. This can be explained by the scattered photon from the liver which interferes the inferior part of heart especially RCA resulting in higher activity. Thus, SUV result shows normal instead of abnormal score. Specificity and accuracy improvement by SUV method of three main vessels (LAD, LCX and RCA) are more significant than sensitivity. It means that SUV method can be used to detect true negative results in myocardial perfusion scan very effectively. From this research, we recommend that visual analysis should still be used and SUV method should be applied to improve specificity. But the SUV of

abnormal scan by using e-soft auto contour can not be used for the clinical application. Because ROI is drawn over the whole left ventricle which includes low uptake and high uptake mixed together. Image J method can be used to determine SUV because it can differentiate each segment of the left ventricle of the heart.

According to anthropomorphic heart and thorax phantom with lesion study, overestimation error was encountered in absent uptake or severe defect for relative percent difference between defect and normal myocardium. That is the reason why the number of positive predictive values decreased and sensitivity is lower than specificity. The overall uncertainties due to measurement errors are a dominant factor for SUV determination in clinical set up. In order to reduce the errors, the incorporation of better imaging models in the reconstruction to allow better compensation for physical effects, patient-induced artifacts (e.g. motion) and proper scatter correction are necessary. New acquisition and processing techniques can help in the future to increase the image information relevant for quantitation and improve the precision(18). The benefit of this study is to obtain absolute quantification for left anterior descending, left circumflex and right coronary vessels of the heart. The severity of defect can be observed by looking at the negative score level.

## 5.2 Conclusion

The objective of this study is to determine Standardized Uptake Value for normal and abnormal patients. The SUV of  $^{99m}\text{Tc}$ -Sestamibi in SPECT/CT for normal myocardial perfusion scan for rest and stress are  $8.03 \pm 1.4$  and  $7.64 \pm 1.5$  in male patients,  $8.26 \pm 0.9$  and  $8.36 \pm 1.5$  in female patients. Using Image J software method, the average SUV for left anterior descending, left circumflex and right coronary artery of the heart in normal myocardial perfusion imaging are  $7.70 \pm 1.2$ ,  $8.15 \pm 1.1$ ,  $7.61 \pm 1.3$  in rest scan and  $7.67 \pm 1.2$ ,  $8.04 \pm 1.5$ ,  $7.56 \pm 1.2$  in stress scan. For abnormal patients, the results showed that SUV has higher negative predictive value for eliminating perfusion defects. Specificity 74%, sensitivity 58% and accuracy 67% of SUV study are higher than conventional myocardial perfusion imaging (51%, 52% and 51%). The conversion factor of cylindrical uniform phantom is 4875

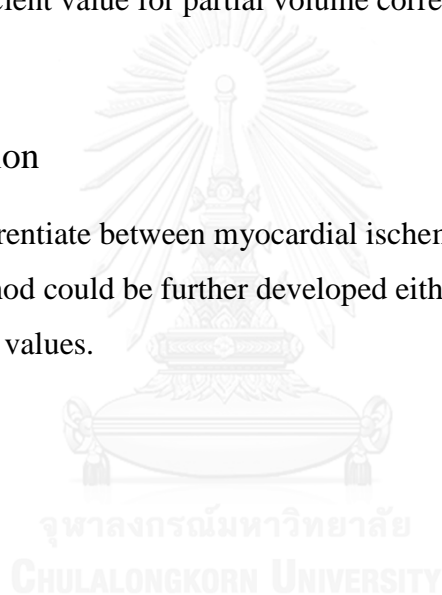
cpm/MBq and recovery coefficient of anthropomorphic thorax and heart phantom is 0.565 from this study. Image J is the best and reliable method to determine SUV result.

### 5.3 Limitations

There are some limitations in this study as the data were retrospectively collected. Radionuclide preparation time, injected dose and acquisition time may be inaccurately recorded. Myocardium perfusion defect size cannot be applied by the exact recovery coefficient value for partial volume correction.

### 5.4 Recommendation

In order to differentiate between myocardial ischemia and myocardial infarction in the future, the method could be further developed either threshold or cut off score that suitable for those values.





## REFERENCES

1. Gaemperli, O, et al. Validation of a new cardiac image fusion software for three-dimensional integration of myocardial perfusion SPECT and stand-alone 64-slice CT angiography. European Journal of Nuclear Medicine and Molecular Imaging 2007;34(7): p. 1097-1106.
2. Sato, A, et al. Quantitative measures of coronary stenosis severity by 64-Slice CT Angiography and relation to physiologic significance of perfusion in nonobese patients: Comparison with stress Myocardial Perfusion Imaging. Journal of Nuclear Medicine 2008;49(4): p. 564–572.
3. Willowson, K, Bailey, DL, Baldock, C. Quantitative SPECT reconstruction using CT-derived corrections. Physics in Medicine and Biology 2008;53(12): p. 3099-3112.
4. Bailey, DL, Willowson, KP. An Evidence-Based Review of Quantitative SPECT Imaging and potential clinical applications. Journal of Nuclear Medicine 2013; 54(1): p. 83–89.
5. Da Silva, AJ, Tang, HR, Wong, KH, Wu, MC, Dae, MW, and Hasegawa, BH. Absolute Quantification of Regional Myocardial Uptake of <sup>99m</sup>Tc-Sestamibi with SPECT: Experimental Validation in a Porcine Model. Journal of Nuclear Medicine 2001;42(5): p. 772-779.
6. Mananga, ES, et al. Myocardial defect detection using PET-CT: Phantom Studies. www.plosone.org 2014; 9(2): e88200.
7. Liu, YH, Sahul, Z, Weyman, CA, Dione, DP, Dobrucki, WL, Mekkaoui, C. Accuracy and reproducibility of absolute quantification of myocardial focal tracer uptake from molecularly targeted SPECT/CT: a canine validation. Journal of Nuclear Medicine 2011;52(3): p. 453-460.
8. Georgosopoulou, M L, et al. Routine quality control recommendations for nuclear medicine instrumentation. European Journal of Nuclear Medicine and Molecular Imaging 2010;37: p. 662– 671.
9. Slart, RH, Tio, RA, Zijlstra, F, and Dierckx, RA. Diagnostic pathway of integrated SPECT/CT for coronary artery disease. European Journal of Nuclear Medicine and Molecular Imaging 2009;36(11): p. 1829-1834.
10. Dvorak, R A, et al. Interpretation of SPECT/CT Myocardial Perfusion Images: Common Artifacts and Quality Control Techniques. www.rsna.org/rsnarights 2011; 31(7): p. 2041–2057.
11. Kalki, K, et al. Myocardial Perfusion Imaging with a Combined X-Ray CT and SPECT System. Journal of Nuclear Medicine 1997; 38(10): p. 1535-1540.
12. Sonesson, H, Engblom, H, Hedstrom, E, Bouvier, F, Sorensson, P, Pernow, J. An automatic method for quantification of myocardium at risk from myocardial perfusion SPECT in patients with acute coronary occlusion. Journal of Nuclear Cardiology 2010;17(5): p. 831-840.
13. Hughes, T, et al. A template-based approach to semi-quantitative SPECT myocardial perfusion imaging: Independent of normal databases. American Association of Physicists in Medicine 2011;38(7): p. 4186-4196.
14. National Electrical Manufacturers Association. NEMA NU 2-2007: Performance Measurements of Positron Emission Tomographs. Rosslyn, VA: NEMA, (2007).

15. Zeintl, J, Vija, AH, Yahil, A, Hornegger, J, Kuwert, T. Quantitative accuracy of clinical  $^{99m}\text{Tc}$  SPECT/CT using Ordered-Subset Expectation Maximization with 3-dimensional resolution recovery, attenuation, and scatter correction. Journal of Nuclear Medicine 2010;51(6): p. 921-928.
16. Leslie, WD, et al. Prognostic Value of Automated Quantification of  $^{99m}\text{Tc}$ -Sestamibi Myocardial Perfusion Imaging. Journal of Nuclear Medicine 2005; 46(2): p. 204–211.
17. Yokota, S, Ottervanger, JP., Mouden, M., Timmer, JR., Knollema, S., Jager, PL. Prevalence, location, and extent of significant coronary artery disease in patients with normal myocardial perfusion imaging. Journal of Nuclear Cardiology 2014;21(2): p. 284-290.
18. Keyes, JW, et al. SUV: Standard Uptake or Silly Useless Value? Journal of Nuclear Medicine 1995; 36(10): p. 1836-1839.



**APPENDIX**



จุฬาลงกรณ์มหาวิทยาลัย  
CHULALONGKORN UNIVERSITY

## APPENDIX A

Patient no.....
Type of scan.....
Sex.....
Age (years).....
Patient weight (g).....
Injected dose (MBq).....
Preparation time.....
Imaging time.....
Activity concentration in region of interest (MBq/cc).....
Standardized Uptake Value.....

Case record form for SUV determination

## APPENDIX B

## Examples of 20 segments SUV by using Image J software

Table 6.1 Rest SUV for abnormal myocardial perfusion scans (patient no.1)

Seg: no.	Area	Total counts	VOL (cc)	Counts /cc	CPM /CC	AcC	AcC (RC)	Inj:act MBq	Bd. Wt.(g)	SUV
1	23	12257	1.96	6269.57	241.14	0.05	0.09	783.1	62000	6.93
2	22	11789	1.87	6304.28	242.47	0.05	0.09	783.1	62000	6.97
3	24	14152	2.04	6937.25	266.82	0.05	0.10	783.1	62000	7.67
4	24	15319	2.04	7509.31	288.82	0.06	0.10	783.1	62000	8.30
5	21	12695	1.79	7112.04	273.54	0.06	0.10	783.1	62000	7.86
6	24	13910	2.04	6818.63	262.25	0.05	0.10	783.1	62000	7.54
7	22	13943	1.87	7456.15	286.77	0.06	0.10	783.1	62000	8.24
8	24	15383	2.04	7540.69	290.03	0.06	0.11	783.1	62000	8.34
9	23	14686	1.96	7512.02	288.92	0.06	0.10	783.1	62000	8.30
10	24	19588	2.04	9601.96	369.31	0.08	0.13	783.1	62000	10.62
11	22	17400	1.87	9304.81	357.88	0.07	0.13	783.1	62000	10.29
12	23	16653	1.96	8518.16	327.62	0.07	0.12	783.1	62000	9.42
13	22	12246	1.87	6548.66	251.87	0.05	0.09	783.1	62000	7.24
14	24	11325	2.04	5551.47	213.52	0.04	0.08	783.1	62000	6.14
15	23	10858	1.96	5553.96	213.61	0.04	0.08	783.1	62000	6.14
16	24	15087	2.04	7395.59	284.45	0.06	0.10	783.1	62000	8.18
17	22	15188	1.87	8121.93	312.38	0.06	0.11	783.1	62000	8.98
18	23	14241	1.96	7284.40	280.17	0.06	0.10	783.1	62000	8.05
19	23	12803	1.96	6548.85	251.88	0.05	0.09	783.1	62000	7.24
20	23	13246	1.96	6775.45	260.59	0.05	0.09	783.1	62000	7.49
									Mean	8.00
									Max	10.62
									Min	6.14

Table 6.2. Stress SUV for abnormal myocardial perfusion scan (patient no.1)

Seg: no.	Area	Total counts	VOL (cc)	Counts /cc	CPM /CC	AcC (MBq/cc)	AcC RC	Inj: act (MBq)	Bd. Wt. (g)	SUV
1	22	6608	1.87	3533.69	135.91	0.03	0.05	624.68	62000	4.90
2	24	6252	2.04	3064.71	117.87	0.02	0.04	624.68	62000	4.25
3	23	9226	1.955	4719.18	181.51	0.04	0.07	624.68	62000	6.54
4	24	14230	2.04	6975.49	268.29	0.06	0.10	624.68	62000	9.67
5	22	15412	1.87	8241.71	316.99	0.07	0.12	624.68	62000	11.42
6	23	13683	1.955	6998.98	269.19	0.06	0.10	624.68	62000	9.70
7	22	12273	1.87	6563.10	252.43	0.05	0.09	624.68	62000	9.10
8	24	10402	2.04	5099.02	196.12	0.04	0.07	624.68	62000	7.07
9	23	11247	1.955	5752.94	221.27	0.05	0.08	624.68	62000	7.97
10	24	18012	2.04	8829.41	339.59	0.07	0.12	624.68	62000	12.24
11	22	16613	1.87	8883.96	341.69	0.07	0.12	624.68	62000	12.31
12	23	16881	1.955	8634.78	332.11	0.07	0.12	624.68	62000	11.97
13	22	12602	1.87	6739.04	259.19	0.05	0.09	624.68	62000	9.34
14	24	12716	2.04	6233.33	239.74	0.05	0.09	624.68	62000	8.64
15	23	11433	1.955	5848.08	224.93	0.05	0.08	624.68	62000	8.11
16	24	17093	2.04	8378.92	322.27	0.07	0.12	624.68	62000	11.61
17	22	15347	1.87	8206.95	315.65	0.06	0.11	624.68	62000	11.37
18	23	14693	1.955	7515.60	289.06	0.06	0.10	624.68	62000	10.42
19	23	10018	1.955	5124.30	197.09	0.04	0.07	624.68	62000	7.10
20	23	10199	1.955	5216.88	200.65	0.04	0.07	624.68	62000	7.23
									Mean	9.05
									Max	12.31
									Min	4.25

## APPENDIX C

### Quality Control of SPECT/CT

#### 1. Part of CT (Daily)

##### Purpose

To check quality of x-ray beam by using water phantom in terms of -

The CT value of water (Hounsfield unit)

The pixel noise of image (standard deviation)

Tube voltage (measure directly on the x-ray tube)

##### Material

Siemens water phantom

##### Methods

1. Warm up CT tube before use on patients. This is necessary because the CT tube needs to be at a particular operating temperature before it performs properly.

2. Then calibrate blank CT for different kVp (80,110 and 130) and mAs (140,150 and 200).

3. Do the same with the water phantom that represent patient tissue equivalent. Draw ROI to evaluate Mean value of CT value and Sigma value (measure for pixel noise).

4. The different image between the first and the second measurement is calculated.

Tolerance level for kVp

For 80 kVp (71.80-87.80)

For 110 kVp (98.80-120.80)

For 130 kVp (116.60-142.60)

Tolerance level for Water value

Voltage: 80 kV

Current: 140 mA

Tolerance:

Slice 1 -1.48...6.52 HU

Slice 2 -2.17...5.83 HU

Slice 3 -1.78...6.22 HU

Voltage: 110 kV

Current: 150 mA

Tolerance:

Slice 1 -2.44...5.56 HU

Slice 2 -2.09...5.91 HU

Slice 3 -2.95...5.05 HU

Voltage: 130 kV

Current: 200 mA

Tolerance:

Slice 1 -2.56...5.44 HU

Slice 2 -2.47...5.53 HU

Slice 3 -3.05...4.95 HU



Tolerance level for Noise

Voltage: 110 kV

Current: 150 mA (14.86....18.16 HU)

Voltage: 130 kV

Current: 200 mA (10.95....13.38 HU)

Table 6. 1 The results of quality daily noise, voltage and water value for a month.

Date	Parameter (KV)	Result voltage (KV)	water value (HU)			Sigma (HU)
			slice 1	slice 2	slice 3	
02.06.14	80	79.8	0.97	0.77	1.12	
	110	109.8	0.19	1.02	-0.08	16.36
	130	129.6	0.2	0.3	-0.23	11.9
03.06.14	80	79.8	1	1.53	0.54	
	110	109.8	0.21	0.04	0.14	16.2
	130	129.8	0.16	-0.38	-0.3	11.85
04.06.14	80	79.8	0.77	-0.31	0.09	
	110	109.8	1.05	-0.24	-0.2	16.17
	130	129.8	0.32	-0.89	-0.14	11.89
05.06.14	80	79.8	1.99	1.9	0.79	
	110	109.6	0.62	0.96	-0.11	16.9
	130	129.8	0.73	-0.11	0.39	11.89
06.06.14	80	79.8	1.27	2.11	0.95	
	110	109.8	0.7	1.03	0.94	16.32
	130	129.8	0.81	0.09	0.08	11.9
10.06.14	80	79.8	0.86	1	0.83	
	110	109.8	0.72	0.11	0.03	16.1
	130	129.6	0.32	-0.01	-0.07	11.85
11.06.14	80	79.8	1.45	0.53	1.04	

	110	109.8	1.02	0.56	-0.28	16.33
	130	129.6	0.42	-0.06	0.15	11.89
12.06.14	80	79.8	1.6	2.04	2.1	
	110	109.8	-0.21	0.5	0.09	16.26
	130	129.6	0.37	0.32	0.1	11.96
13.06.14	80	79.8	1.51	0.75	1.6	
	110	109.8	0.58	0.44	0.01	16.29
	130	129.4	0.45	-0.2	-0.18	11.86
16.06.14	80	79.8	2.21	1.61	0.92	
	110	109.8	1.06	0.78	0.02	16.16
	130	129.8	0.58	0.1	0.19	11.91
17.06.14	80	79.8	1.04	1.91	0.98	
	110	109.8	0.63	0.6	0.22	16.34
	130	129.6	0.15	-0.47	0.47	11.93
18.06.14	80	79.8	1.32	1.15	0.55	
	110	109.8	0.63	0.28	-0.3	16.24
	130	129.4	0.62	0.02	0.18	11.98
19.06.14	80	79.8	0.63	0.62	1.79	
	110	109.8	0.58	0.76	0.61	16.23
	130	129.6	0.37	0.25	0.14	11.88
20.06.14	80	79.8	1.72	0.11	1.04	
	110	109.8	1.43	-0.65	0.12	16.28
	130	129.6	0.66	-0.16	-0.08	11.99
23.06.14	80	79.8	2.07	0.37	0.83	
	110	109.8	0.8	0.39	0.29	16.21
	130	129.6	0.5	0.11	0.6	11.91
24.06.14	80	79.8	1.73	1.66	0.23	
	110	109.8	0.38	0.34	0.64	16.33
	130	129.6	0.78	0.19	-0.15	11.93
25.06.14	80	79.8	0.36	2.01	1.16	
	110	109.8	0.93	0.3	0.65	16.38
	130	129.6	0.22	0.18	0.56	12.01

26.06.14	80	79.8	0.2	1.77	1.87	
	110	109.8	1.38	0.42	0.56	16.21
	130	129.6	0.94	-0.21	-0.24	11.83
27.06.14	80	79.8	2.18	2.4	0.58	
	110	109.8	0.98	0.66	0.76	16.23
	130	129.6	0.17	0.33	0.29	11.93
30.06.14	80	79.8	1.29	1.04	0.79	
	110	109.8	0.41	0.57	0.08	16.08
	130	129.8	0.82	-0.42	0.21	11.89

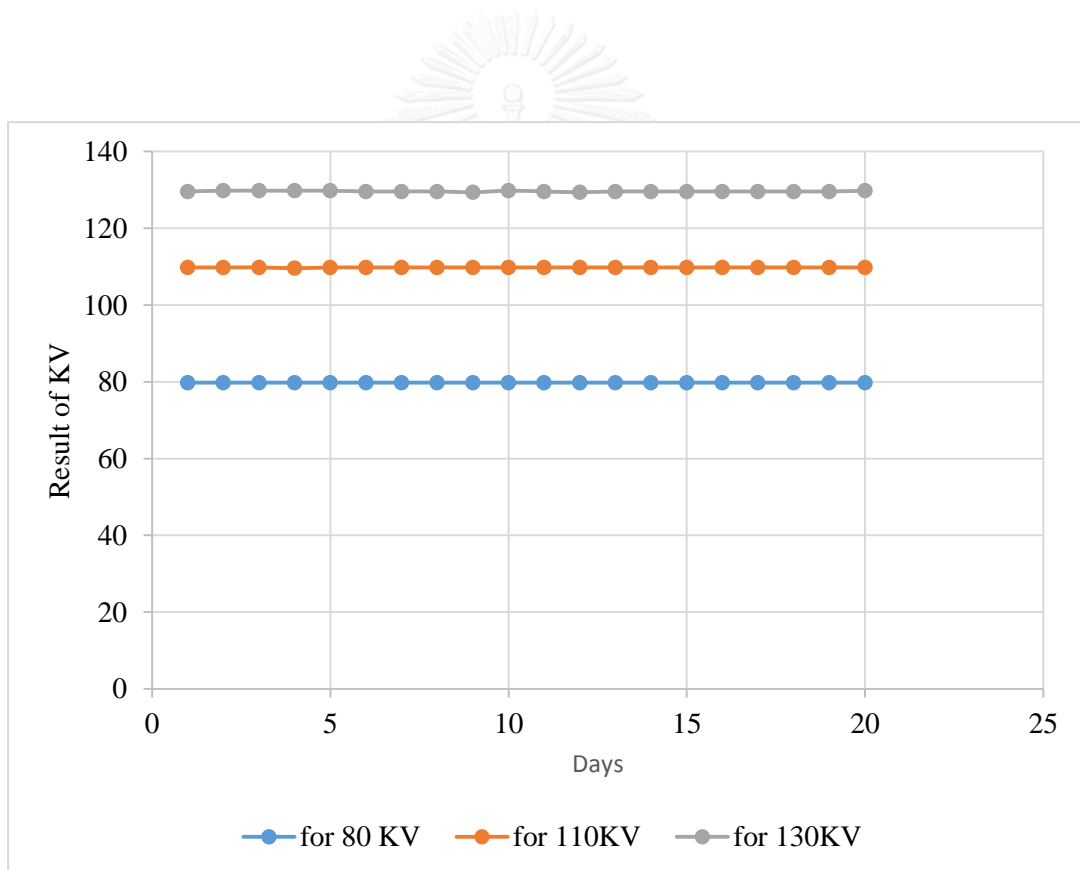


Figure 6.1 The result of CT Voltage for one month

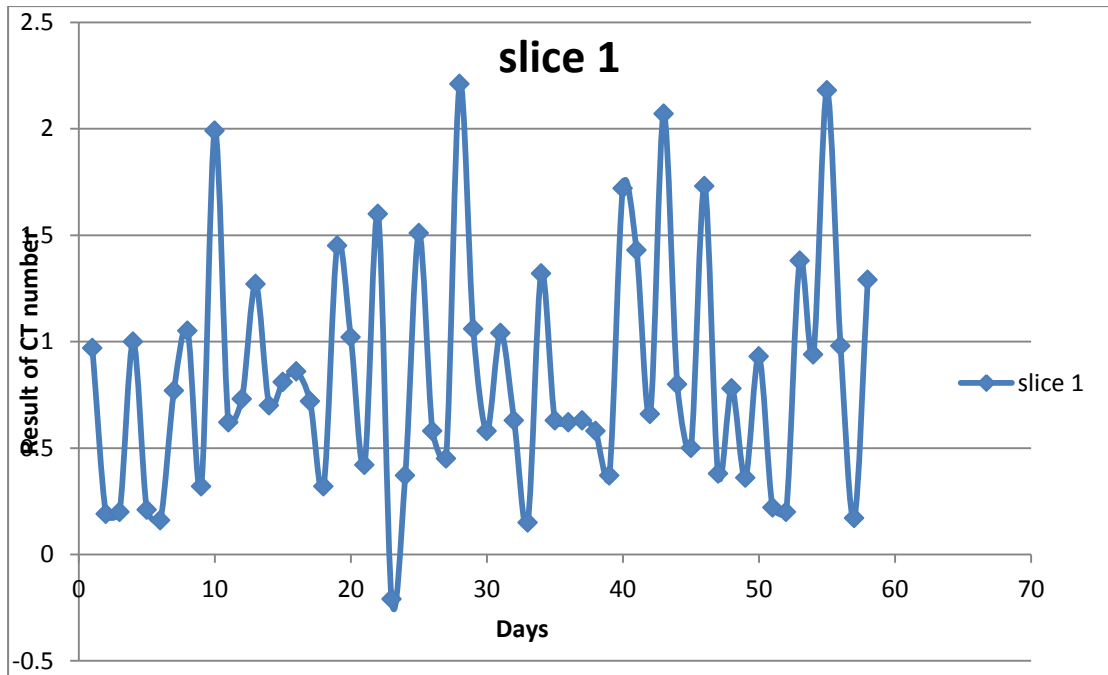


Figure 6.2 The result of CT water value for one month for slice 1

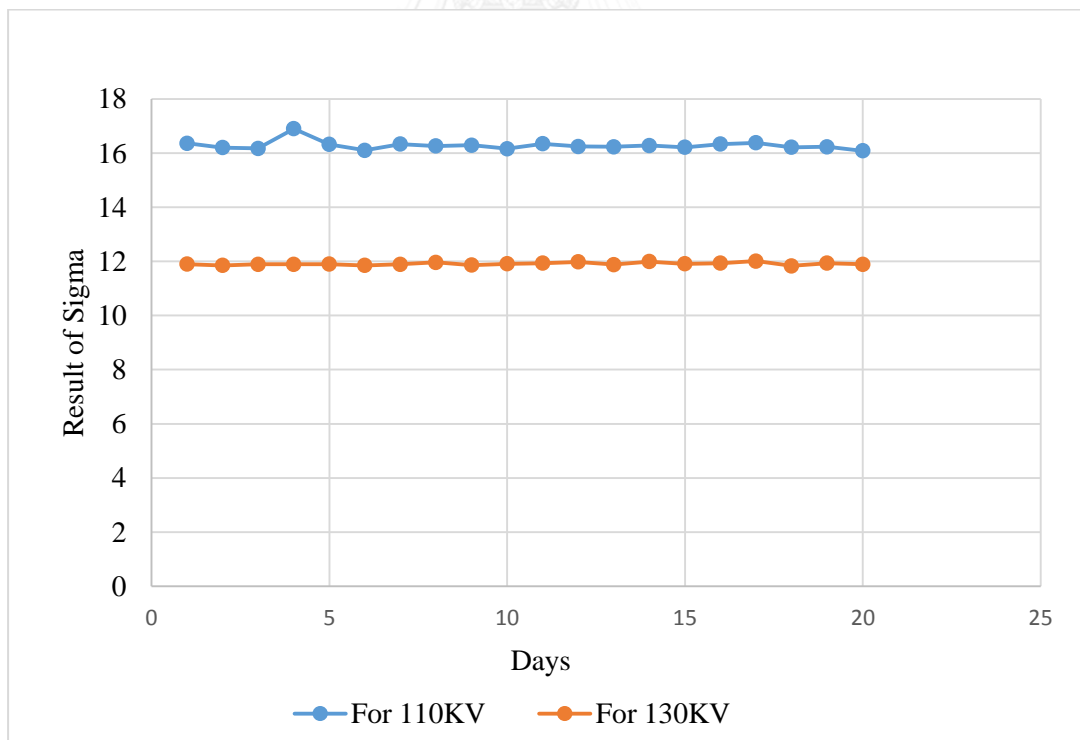


Figure 6.3 The result of noise for 110 KV and 130 KV for one month  
Comment: Pass

## 2. Part of SPECT

### 2.1 Weekly Intrinsic uniformity calibration

#### Purpose

To check the intrinsic response of a scintillation camera to a spatially uniform flux of incident photons over the field of view using a symmetric (centered) energy window over the photo peak(8).

To update intrinsic flood uniformity Calibration database

#### Materials

1. Point source consists of 20 uCi Tc-99m solution in suitable container.
2. Source holder for point source.

#### Methods

1. Remove the collimator from the detector head. Align the detector head and source holder.
2. Mount the source in the source holder.
3. Use weekly QC protocol for peaking, tuning and acquiring 30M counts.
4. Center the clinically used window on the photo peak.

Differential uniformity: the amount of count density change per defined unit distance when the detector's incident gamma radiation is a homogeneous flux over the field of measurement.

$$\text{Differential Uniformity} = \pm 100 * ((\text{Max} - \text{Min}) / (\text{Max} + \text{Min}))$$

Integral uniformity: a measure of the maximum count density variation over a defined large area of the scintillation detector for a uniform input gamma flux to the Useful Field of View of the camera.

$$\text{Integral Uniformity} = \pm 100 * ((\text{Max} - \text{Min}) / (\text{Max} + \text{Min}))$$

## Results:

Peak of both detector for Tc-99m is 141.35 KeV.

Tuning is passed for both detectors.

Table 6. 2 Weekly intrinsic uniformity results for one month

Date	Uniformity Detector 1				Uniformity Detector 2			
	CFOV		UFOV		CFOV		UFOV	
	IU	DU	IU	DU	IU	DU	IU	DU
6.5.2014	1.74	1.14	2.57	1.41	1.79	1.06	1.91	1.06
12.5.2014	1.68	1.01	1.82	1.67	1.39	1.17	1.64	1.17
19.5.2014	1.71	1.39	2.06	1.39	1.69	1.2	1.96	1.8
26.5.2014	1.77	1.23	2.14	1.4	1.57	1.14	1.9	1.74

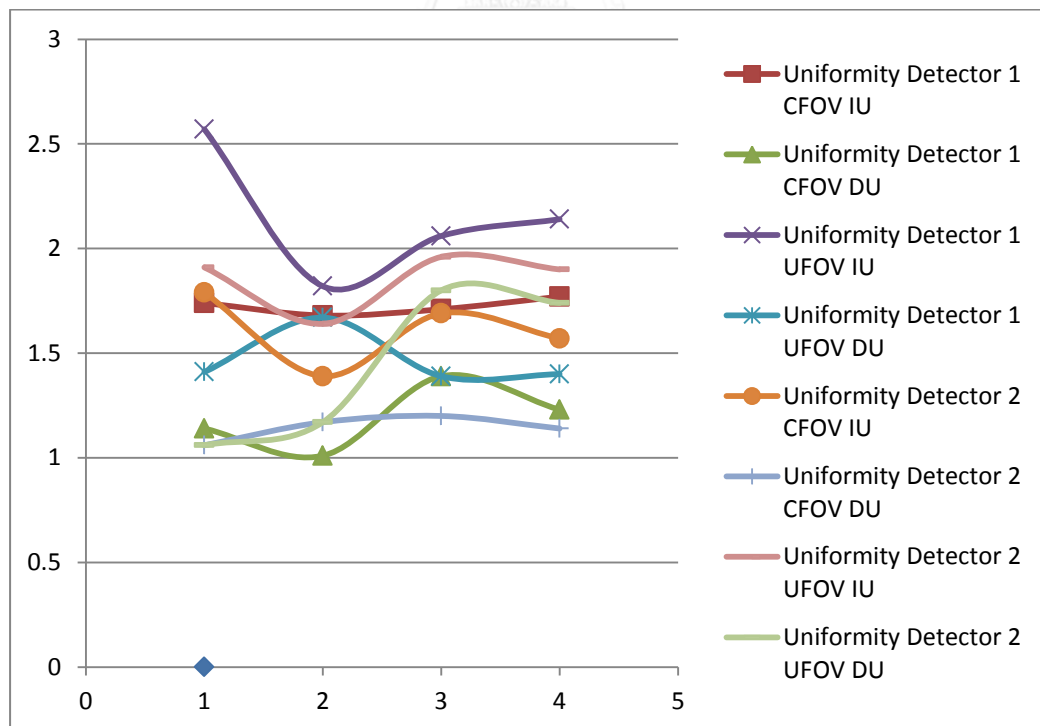


Figure 6.4 Weekly intrinsic uniformity graph for a month

## NEMA tolerance level for Uniformity

	CFOV	UFOV
Integral	$\pm 2\%$	$\pm 2.5\%$
Differential	$\pm 1.5\%$	$\pm 2\%$

Comment: Pass

## 2.2. Energy window check (Peaking)

## Purpose

To check the correct energy setting (i.e. a photo peak in the center of the energy window).

## Materials and Methods

The same as the monthly intrinsic uniformity

Use daily QC protocol for peaking and acquiring 30M.

## Results

Table 6. 3 Daily energy peaking results for one month

Date	Energy peak	
	Det1	Det2
1/5/2014	141.35	141.35
2/5/2014	141.35	141.35
6/5/2014	141.35	141.35
7/5/2014	141.35	141.35
8/5/2014	141.35	141.35
12/5/2014	141.35	141.35
14/5/2014	141.35	141.35
15/5/2014	141.35	141.35
16/5/2014	141.35	141.35
19/5/2014	141.35	141.35
20/5/2014	141.35	141.35
21/5/2014	141.35	141.35
22/5/2014	141.35	141.35
23/5/2014	141.35	141.35

25/05/2014	141.35	141.35
26/05/2014	141.35	141.35
27/05/2014	141.35	141.35
28/05/2014	141.35	141.35
29/05/2014	141.35	141.35
30/05/2014	141.35	141.35

Comment: Pass

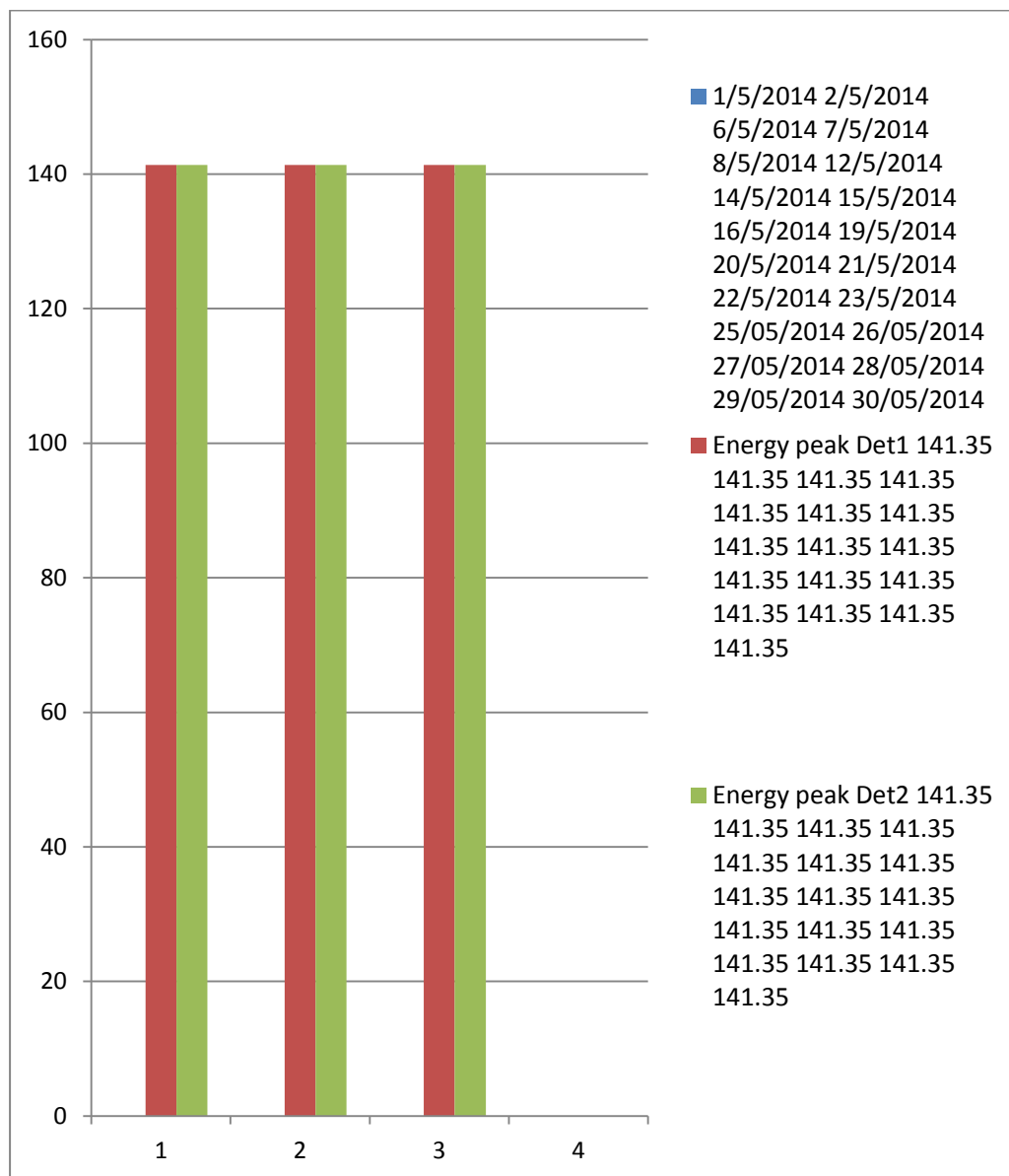


Figure 6.5 Daily energy peaking graph for a month



### 2.3. Center of rotation

#### Purpose

To check the center of rotation offset, alignment of the camera Y-axis and head tilt with respect to the axis of rotation.

#### Materials

Five  $^{99m}\text{Tc}$  point sources

MHR/COR phantom

#### Methods

1. Prepare 5 point sources with activity approximates 37 MBq on the vial supplied with camera system
2. Mount the vial source on MHR/COR phantom and place on top of the patient bed.
3. Reconfigure the detectors with LEUR collimator to 180-degree configuration and make sure that 5 point sources are in center of field of view.
4. Rotate detector to 90 degree to check that 5-point source are at center.
5. Use MHR/COR protocol to perform acquisition with non-uniformity correction.
6. Perform MHR/COR calibration on detector 90 degree configuration

#### Results

Table 6. 4 MHR/COR for 180 degree detector configuration result

	Detector 1	Detector 2
COR	2.142 mm	-0.604 mm
Axial shift	0.224 mm	-0.224 mm
Back projection angle	0.042 degree	-0.042 degree
System resolution at 20cm	11.480 mm	11.580mm

Table 6. 5 MHR/COR for 90 degree detector configuration result

	Detector 1	Detector 2
COR	4.485 mm	-3.340 mm
Axial shift	0.311mm	-0.311mm
Back projection angle	0.093 degree	-0.093degree
System resolution at 20cm	12.386 mm	12.387mm

#### Limits of acceptability

The mean value of center of rotation offset should be  $< 10$  mm and the back projection angle should be  $< 0.8$ . Axial shift should be  $< 5$ mm.

Comment: MHR/COR results are within limit.

## 2.4. Whole-body System Spatial Resolution

### Purpose

To measure system spatial resolution parallel and perpendicular to the direction of motion

To avoid loss of resolution in the scanning direction during whole body scans

### Materials

Four capillary tubes with high concentration of  $^{99m}\text{Tc}$  (not greater than 20kcps), LEUR collimators.

### Methods

1. Fill  $\text{Tc-}^{99m}$  pertechnetate into the four capillary tubes with high concentration that count rate is not greater than 20kcps.

2. Place a pair of capillary tubes, which 10 cm distance parallel to direction of motion.
3. Place another pair of capillary tubes perpendicular to the direction of motion which one capillary tube on center of table.
4. Acquire Whole body image with matrix 256x1024, speed 10 cm/min, minimum distance between detector and line source.

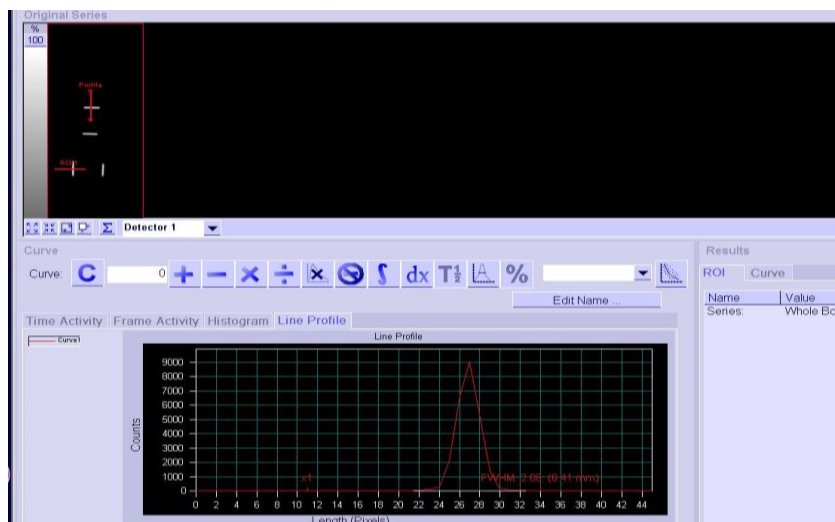


Figure 6.6 Line profile to measure FWHM

Table 6. 6 FWHM result for Whole-Body system spatial resolution parallel and perpendicular to the direction of motion

Direction	Detector 1			Detector 2		
	FWHM (mm)			FWHM (mm)		
	Line 1	Line 2	Average	Line 1	Line 2	Average
Perpendicular	6.35	6.10	6.225	7.21	6.78	6.995
Parallel	6.19	5.58	5.885	6.84	6.64	6.74

Comment: Detector 1 shows the better resolution than detector 2 because the distance of detector 2 is further than detector 1 and table attenuation

## 2.5. System Spatial Resolution with scatter

### Purpose

To test the system spatial resolution of a scintillation camera in terms of the full width at half maximum (FWHM) of its line-spread function

### Materials

JASZCZAK Phantom

Three capillary tubes with high concentration of  $^{99m}\text{Tc}$

### Methods

1. Place the three sealed capillary tubes at the appropriate position inside the JASZCZAK phantom filled with water.
2. Put the phantom on top of the patient bed.
3. Acquire counts with LEUR collimator, matrix size 128x128, zoom 1 and 15 sec/view for 30 views.
4. Use SPECT Tomo protocol.

### Results

Table 6. 7 FWHM result for system spatial resolution with scatter

	At center	Rt. offset	Lt. offset
Spatial resolution	10.05	9.84	9.95
(mm)	10.01	9.76	9.84

## 2.6. System Planar Sensitivity

### Purpose

To test the count rate response of a scintillation camera to a radionuclide source of known radioactivity

### Materials

A petri dish with 10 cm diameter

A foam with 10 cm height

### Methods

1. Fill water 20 cc and 99mTc activity 80.512MBq into the petri dish.
2. Place the foam on the center of detector and put on petri dish on top.
3. Acquire counts for five minutes with LEUR collimator, matrix 256x256, zoom 1, no uniformity correction.
4. Perform the acquisition with both detectors and record the total counts for each detector.

Table 6. 8 The results of Collimator LEUR for Tc-99m

	Detector 1	Detector 2	<b>Specification</b>
Counts/5min	964826	964333	
Cps/mCi	1482.7	1482	
Cpm/uCi	88.9	88.9	<b>101</b>

Comment: Detector 1 and 2 has the same sensitivity and the results are lower than specification. It is within the acceptable limit.

## VITA

NAME	Miss Ohnmar Swe
SEX	Female
NATIONALITY	Myanmar
DATE OF BIRTH	14 November 1976
PLACE OF BIRTH	Bago Division, Myanmar
INSTITUTIONS ATTENDED	Institute of Paramedical Science (Yangon), 2001: Bachelor of Paramedical Science (B.P.Sc) University of East Yangon, 2010: Bachelor of Science (Physics) Q
POSITION HELD & OFFICE	Nuclear medicine Technologist, 2002 to present Department of Nuclear Medicine Yangon General Hospital Yangon, Myanmar
HOME ADDRESS	F-2, Room no. 207, Shu Khinn Thar Housing, Thaketa Township, Yangon, Myanmar